

FREQUENCY AND TERRAIN FACTORS FOR HIGH-FREQUENCY SNOW
AVALANCHE PATHS

by

MICHAEL JOHNSON SMITH

B.Sc, The University of Wales, 1993

A THESIS SUBMITTED IN PARTIAL FULFILLMENT OF
THE REQUIREMENTS FOR THE DEGREE OF
MASTER OF SCIENCE

in

THE FACULTY OF GRADUATE STUDIES
(Department of Geography)

We accept this thesis as conforming
to the required standard

.....

.....

.....

.....

THE UNIVERSITY OF BRITISH COLUMBIA

July 1995

© Michael Johnson Smith, 1995

ABSTRACT

The expected frequency of avalanche events is an essential component of risk in land-use planning and design of avalanche defences in the runout zone. In the past, detailed field studies have been undertaken to determine the frequency of avalanches on individual paths, but there have been few studies to determine the frequency analytically from terrain variables or to determine a probability distribution from which formal risk calculations can be made.

In this thesis, I present an analysis based on intensive field measurements for high-frequency avalanche paths (return period less than 30 years). My study focuses on two important aspects:

- (1) calculation of extreme runout on high-frequency avalanche paths using terrain variables.
- (2) determination of the probability-density or probability-mass function for high-frequency avalanche paths as an input to risk assessment.

By virtue of the extensive database, the work in this thesis represents the most comprehensive study of high-frequency avalanche paths now in existence. The results will find application in land-use planning studies, risk mapping calculations and design of avalanche defences.

TABLE OF CONTENTS

ABSTRACT	ii
LIST OF TABLES	vi
LIST OF FIGURES	vii
ACKNOWLEDGEMENTS	x
1. INTRODUCTION	1
1.1 A RATIONALE FOR STUDY	1
1.2 AVALANCHES AND AVALANCHE TERRAIN	4
1.3 TERRAIN AND LAND MANAGEMENT	6
1.4 CONCLUSIONS	7
2. PREDICTION OF EXTREME RUNOUT	9
2.1 INTRODUCTION	9
2.2 RUNOUT PREDICTION	9
2.2.1 Introduction	9
2.2.2 Physical Models	10
2.2.3 Bovis and Mears (1976)	11
2.2.4 Lied and Bakkehøi (1980)	12
2.2.5 McClung and Lied (1987)	14
2.3 AVALANCHE ZONING	15
2.3.1 Avalanche Zoning Schemes	15
2.3.2 Use of Statistical and Physical Models	16
2.3.3 Conclusion	17

3. AVALANCHE MAGNITUDE AND FREQUENCY	19
3.1 INTRODUCTION	19
3.2 AVALANCHE MAGNITUDE AND FREQUENCY	20
3.2.1 Fitzharris (1977)	20
3.2.2 Föhn (1975)	21
3.3 CLIMATE AND AVALANCHE FREQUENCY	21
3.4 CONCLUSIONS	22
4. TERRAIN ANALYSIS	23
4.1 INTRODUCTION	23
4.2 DESCRIPTION OF METHODS	24
4.2.1 Selection Criteria	24
4.2.2 Measurement Procedures	24
4.2.3 Problems Encountered	25
4.2.4 Air Photo Interpretation and Digitizing	27
4.2.5 Curve Fitting	29
4.3 DATA ANALYSIS	32
4.3.1 Descriptive Statistics and Comparison with Past Results	32
4.3.2 Regression Models	35
4.3.3 Extreme-Value Models	37
4.3.4 Outliers	39
4.4 CONCLUSIONS	42
4.4.1 Data Collection	42
4.4.2 Results	43

5. STUDY OF ARRIVAL RATE	45
5.1 INTRODUCTION	45
5.2 DESCRIPTION OF ROGERS PASS AND DATA	46
5.3 FREQUENCY ANALYSIS - GOODNESS OF FIT	47
5.4 RELATION BETWEEN FREQUENCY AND TERRAIN PARAMETERS	51
5.5 DISCUSSION AND CONCLUSIONS	56
6. CONCLUSIONS	62
6.1 INTRODUCTION	62
6.2 THESIS REVIEW	62
6.3 FINAL REVIEW AND RECOMMENDATIONS	66
NOMENCLATURE	68
BIBLIOGRAPHY	69
APPENDIX 1 - FIELD REPORT	74
APPENDIX 2 - AVALANCHE PATHS AND PHOTOGRAPHY	77
APPENDIX 3 - SUMMARY STATISTICS FOR LOW-FREQUENCY AVALANCHE PATH REGIONS	79

LIST OF TABLES

Table 4.1	<p>ΔX values from field measurements and regression estimates. The top half of the table contains paths $-\Delta X$ and the bottom half $+\Delta X$ values (units are in meters). Note the poor estimates of ΔX for both orthogonal and regression methods when compared to field measurements.</p>	30
Table 4.2	Descriptive statistics of parameters for the Columbia Mountains.	34
Table 4.3	Descriptive statistics of the terrain variables used in the regression analysis. See text for definition of categorical variables denoted by (*).	36
Table 5.1	Frequency table of chi-square test passes and fails (at 0.05 significance) using the equal-interval method, by avalanche path frequency, for normal, Poisson and chi-square distributions.	50
Table 5.2	Predictor variables and descriptive statistics of data used in the regression analysis. See text for definition of categorical variables denoted by (*).	50
Table A2.1	Avalanche paths used in terrain analysis and their respective photography	
W	Whitewater (5c) KP Kootenay Pass (8)	
GF	Grand Forks North (4a) GP Galena Pass (9b)	
BP	Blueberry-Paulson (4b) RP Rogers Pass (22)	
MD	Mica Dam (9a) TC Toby Creek (11b)	
ND	New Denver-Kaslo (7a) G Glacier (10a)	78
Table A3.1	Summary statistics for low-frequency avalanche path regions, with the notation	
CR	Canadian Rockies WN western Norway	
CA	Coastal Alaska CoR Colorado Rockies	
SN	Sierra Nevada BC British Columbia Coast Mountains	
M	south-west Montana	80

LIST OF FIGURES

Figure 1.1 Morphological units of an idealized avalanche path.	3
Figure 2.1 Geometry variables of an avalanche path used in extreme-runout analyses (Nixon and McClung, 1993).	13
Figure 2.2 Runout ratio fitted to extreme value probability distribution for five mountain ranges. (◇) Sierra Nevada, (×) Colorado Rockies, (+) coastal Alaska, (Δ) Canadian Rockies, (□) western Norway (McClung and Mears, 1991). . . .	13
Figure 4.1 Frequency histogram for values of ΔX	30
Figure 4.2A Example of digitized centre line plotted as a profile for Path 55.7 at Toby Creek	31
Figure 4.2B Example of digitized centre line plotted as a profile for Path 21.7 at Kootenay Pass	31
Figure 4.3 Plot of α against β	36
Figure 4.4 Aspect of avalanche paths, using 16 ordinal units, with N=1, S=9, E=5 and W=14 (chosen for graphical reasons). Note the high clustering of values around south.	40
Figure 4.5 Frequency histogram of the runout ratio using the method of lengths . . .	40
Figure 4.6 Gumbel plot of runout ratio data for the Columbia Mountains.	41
Figure 4.7 Gumbel plot of ΔX (units are in meters) data for the Columbia Mountains.	41
Figure 5.1A Avalanche frequency for Cougar Corner 2 (light) fitted to a Poisson distribution (dark). This path has a frequency of 10.1 events per year. Results of Chi-square test were: Degrees of Freedom 7, Chi-Square Statistic 2.55 and Significance Level 0.923	49

Figure 5.1B Avalanche frequency for Tupper Cliffs fitted to a Poisson and normal distribution. This path has a frequency of 6.2 events per year. Results of Chi-square test:

	Normal	Poisson	
Degrees of Freedom	7	7	
Chi-Square Statistic	8.30	18.5	
Significance Level	0.307	0.010	49

Figure 5.2 Location of avalanche paths at Rogers Pass with respect to avalanche frequency. Location is calculated as distance (km) east-west of the Rogers Pass summit (designated as 0) where the centre of the path dissects the Trans-Canada Highway. Negative location is east of Rogers' Pass and positive is west. 58

Figure 5.3 30 year maximum water equivalent plotted against avalanche frequency. Maximum snow depth measurements at 6 different elevations on the east and west side of Rogers Pass are highly correlated with elevation. This relationship is used to calculate the maximum water equivalent for the centre of the catchment for each path and then, using a cube root normal distribution, the 30 year maximum is calculated. 58

Figure 5.4 Wind Index plotted against avalanche frequency, where the Wind Index is a qualitative index of the magnitude of snowdrifting that can be expected in the avalanche starting zone. 59

Figure 5.5 Roughness as a function of avalanche frequency, where roughness is the water equivalent of snow required to cover rocks, shrubs and ledges before avalanches will run. A negative correlation is displayed here: as the roughness in the starting zone increases, so the frequency decreases. 59

Figure 5.6 Aspect of avalanche paths, using 16 ordinal units. Note the high clustering of values around south and north. For the regression analysis, each path was assigned a categorical value of either northerly or southerly.	60
Figure 5.7 Plot of the residuals versus the predicted values for the stepwise multiple regression, using avalanche frequency as the dependent variable. The pattern indicates that the variance of the multiple regression residuals is not constant.	60
Figure 5.8 Plot of the residuals versus the predicted values for the stepwise multiple regression, using a log transformation of the avalanche frequency as the dependent variable.	61
Figure A1.1 Location of field checked avalanche areas, monitored by the Ministry of Transportation and Highways or Parks Canada, within south-west British Columbia	76

ACKNOWLEDGEMENTS

To my son Ieuan, to whom I would like to dedicate this work; he will be a pleasurable reminder of my time here at UBC.

I would like to thank Dr Dave McClung for his thought provoking ideas and constance as my supervisor throughout this work. Many of the ideas here are his and bear fruit from his work in the 1980's. His practical mind and "hard ball" approach to research have sharpened my work and made me a better researcher.

I am very grateful to my wife, Cathy, who endured countless hours of unresponsiveness while I played on the computer, as well as making many meals and cups of tea! She also acted in the role of statistical consultant and general mathematics tutor, getting me though those bleak periods when I started sleeping, eating and dreaming equations. She has left her indelible mark on this thesis.

I would like to thank Peter Schaerer for data used in this thesis, as well as lending his personal knowledge of Rogers' Pass. Many thanks to Jonathon Henkelman for writing the chi-square testing programme and Arnold Moys for many helpful hours instructing me in the use of the AP190 stereo-plotter. Thanks to Dr Othmar Buser of the Swiss Federal Institute for Snow and Avalanche Research, for advice and information. Dr John Lane from the Department of Statistics, University of Wales, Aberystwyth also provided valuable information on testing small samples of data.

I am also grateful to the avalanche control personnel members of Glacier, Banff and Jasper National Parks for their personal knowledge of their respective areas. The Ministry of Transportation and Highways, particularly the avalanche section in Victoria, provided essential data and information on many of the avalanche paths in the current data set.

This work was supported by the Natural Science and Engineering Research Council of Canada and a Teaching Assistantship from the Geography Department at UBC.

1. INTRODUCTION

1.1 A RATIONALE FOR STUDY

With the expansion of settlement into the mountain environment, knowledge about natural hazards is becoming more important. To be able to safely interact with this environment an understanding of those processes operating and their respective risks is necessary. Snow avalanches have become increasingly important in alpine regions as pressure to expand has forced development into mountainous areas. Many European countries have, for several centuries, seen increasing pressure for permanent residence as well as recreation in these regions. Other areas of the world are beginning to feel similar expansion. Perhaps one of the greatest pressures in North America is that of transport links. Often the quickest route is over mountainous terrain and, as in Western Canada, avalanche terrain is traversed.

Initial research on the management of avalanche terrain focused on the mathematical modelling of avalanches (eg Voellmy, 1955). However, it has proved difficult to produce consistent results due to the need to estimate certain boundary conditions. More recently, statistical approaches in conjunction with physical models, have allowed the definition of runout distances of avalanches and so their velocity and impact pressures. Other work has also been concerned with estimating the mass of snow for a coming winter given certain predictor variables. These different approaches can be used in hazard zoning with respect to the maximum avalanche, as well as in the assessment of appropriate defences and their design (height, strength etc). They also permit budgeting for the estimated magnitude of avalanching in a given season.

Most previous work on avalanche runout prediction has been primarily concerned with

low-frequency "limit" avalanches. Databases of avalanche paths are based on low-frequency paths in order to delimit maximum runouts and consequently velocities and impact pressures. In terms of defining hazardous and potentially hazardous terrain this is effective; however, very little work has concentrated on the features and characteristics of high-frequency avalanche paths. Risk from natural hazards may be thought of in terms of consequences, chance of occurrence and exposure in time and space. Risk can be defined in a probabilistic sense in terms of the product of three parameters:

$$P_s = P_v \times P_h \times P_e$$

where P_s is specific risk, P_v is vulnerability, P_h is the frequency (reciprocal of the return period) and P_e is exposure. P_v and P_e tend to change very little from one path to another (perhaps one order of magnitude), while P_h can change over many orders of magnitude. This characteristic is often noticeable in risk studies, as changes in risk are primarily due to changes in event frequency (see §3.1 for a more detailed discussion on risk probabilities). Thus many management decisions in avalanche terrain will be concerned with high-frequency avalanching. Given the importance of high-frequency avalanche paths it is surprising that little work has been accomplished on this area.

There are two separate aspects of high-frequency avalanching, important for land management, that I focus upon in this thesis. The first is a study of extreme runout of high-frequency avalanche paths. I have compiled a database of 46 high-frequency avalanche paths in the Columbia Mountains, British Columbia, whose extreme runout could be measured, and have performed statistical analyses in order to estimate extreme runout. Recommendations are made for the calculation of extreme runout of high-frequency paths in avalanche zoning exercises.

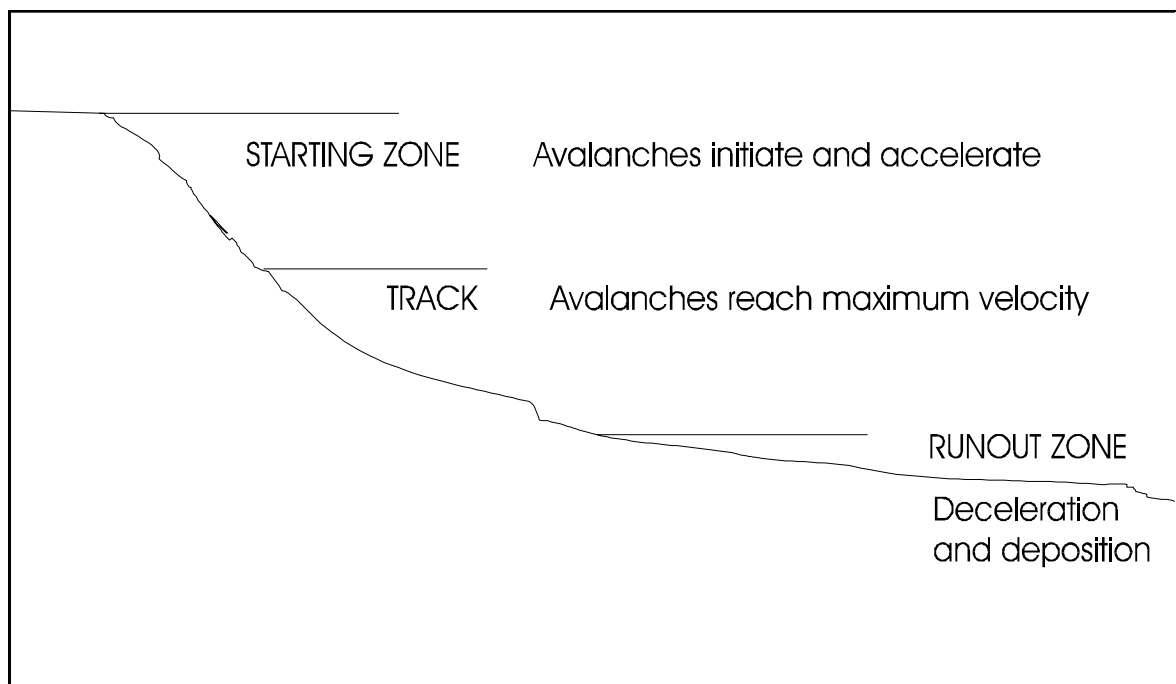


Figure 1.1 Morphological units of an idealized avalanche path.

The second area of study uses a database of 24 years of avalanche occurrence records from Rogers' Pass, British Columbia, to test the applicability of probability distributions in risk assessment. I also performed a detailed analysis of terrain features with respect to avalanche event frequency for individual avalanche paths.

Information on extreme runout, the use of probability distributions in risk mapping and the relationship of avalanche frequency to terrain characteristics are essential for the management of avalanche terrain. Given the importance of high-frequency avalanching, and the further encroachment of people into mountainous regions, this work is valuable for allowing safe occupancy of otherwise dangerous terrain.

1.2 AVALANCHES AND AVALANCHE TERRAIN

Avalanche paths can be divided into three morphologic units (see Figure 1.1). These are broadly termed the starting zone, the track and the runout zone.

The **starting zone** ($\approx 30\text{-}50^\circ$) is where avalanches are released and then accelerate. Starting zone slope angle is the most important variable for avalanche initiation. However, high elevation forest can prevent the build up of snow, especially wind slab. Removal of forests would create new initiation zones as well as reducing the anchoring effect of trees. Other secondary effects include the roughness of the area; once covered by snow, rough elements no longer have an anchoring effect. Starting zone aspect influences the development of the snowpack through the amount of exposure to the sun.

The **track** ($\approx 30\text{-}15^\circ$) is the slope below the starting zone and connects the starting zone to the runout zone. Avalanches attain their maximum velocities here. There can be either entrainment or deposition of material depending on the type and size of avalanche. The track may be open or channelized.

The **runout zone** ($<15^\circ$) is where rapid deceleration of the avalanche occurs and material is deposited. Forest stands can provide buffer zones for slopes lower down. The variable configurations of these three zones will influence the type and frequency of avalanching at a particular site.

In this section I summarise work on avalanche terrain. Much work has been concerned with the prediction of extreme avalanche runout, with an analysis of avalanche terrain as a secondary consideration. These studies are reviewed in Chapter 2 and directly compared to the results in Chapter 4. One area that has seen detailed work is Rogers' Pass, British Columbia. Avalanche occurrences have been monitored since 1967 and consequently the area has been the focus of much work relating to frequency, magnitude and terrain

analyses.

Schaerer's pioneer work at Rogers' Pass was concerned with estimating avalanche magnitude and frequency from terrain and climate variables. He realised that terrain and climate have complex interactions that produce the observed record of magnitude and frequency. Regionally, climate is the most important variable affecting frequency; however on a local scale there more intricate interactions between micro-climate and terrain. In Chapter 5 I look at how terrain features effect avalanche frequency, introducing surrogate variables for climate to provide additional explanation of variations in frequency.

Initial research at Rogers' Pass was concerned with the safety of the Trans-Canada Highway as it traversed the pass. Although research had been carried out on the most effective defensive measures, avalanches still caused many problems. Early papers (Schaerer, 1967) focused on the relationship of terrain and climate variables to avalanche snow yield. Schaerer (1973) went on to estimate the frequency of avalanches on individual paths. Track angle was found to be the most important parameter related to frequency. Schaerer went on to use the height and age of trees in the avalanche runout zone to estimate the frequency. This demonstrated that the greater the forestry cover, the lower the frequency.

Schaerer (1977) also discussed the actual types of terrain associated with different avalanche frequencies. A correlation matrix pointed to the most significant variables for use in a multiple-regression analysis. Conditions at the fracture point appeared to be of most significance. Various conclusions were drawn on snow drifting, gradient of track, gradient of fracture point, roughness, track confinement and aspect. This method was later extended (Schaerer, 1988) by performing a multiple regression analysis on the yield of snow on individual avalanche paths, using climate and terrain predictor variables. In a broad relation to magnitude, he defined the **Yield Ratio** (see Nomenclature) as the proportion of the yield

of snow to total snow available. This gave a yearly ratio of 11.24%, while a 30 year maximum was calculated to be 38.6%. The effect of artillery control of avalanches at Rogers Pass was to increase the ratio, but mainly through small magnitude events. Schaerer suggested that terrain variables have a stronger influence on yield than climate variables.

McGregor (1989) studied the effect of terrain variables on avalanche formation processes and occurrence in South Island, New Zealand. He identified four starting zone types and three different track types. Mean track angles were relatively steep (29.5°), denoting short, steep scree slopes. Runout zones were also relatively steep (20°). The avalanche terrain reflected the effects of postglacial fluvial and mass movement processes on highly fractured greywacke. Of particular interest were the runout zones on steeply inclined (up to 25°), densely vegetated slopes. Avalanches were seen to penetrate over 50m into the forest stands. McGregor also found starting zone morphology and aspect instrumental in determining the avalanche type and frequency.

1.3 TERRAIN AND LAND MANAGEMENT

Mears (1979,1992), in discussing avalanche **return periods** (see Nomenclature), suggested that the size and length of the runout zone could be used to establish relationships with magnitude and frequency. These could then be used to designate a **design-avalanche magnitude** (see Nomenclature) for different land users. He defined a practical upper limit as the 100-year return period and emphasised that different types of extreme avalanche events (dry powder snow, wet snow) would often take divergent routes across the runout zone.

The **encounter probability** (see Nomenclature) can be constructed from an understanding of the magnitude and frequency characteristics of an avalanche path. The encounter probability is used in risk calculations to define P_h (frequency); Chapter 5 is concerned with determining the best frequency distribution to be used when calculating the

encounter probability. At lower elevations on the avalanche path the frequency decreases; however the magnitude is likely to increase. Thus an extreme avalanche (high magnitude) is likely to be a low-frequency event. McClung and Schaerer (1993) state that avalanche frequency is primarily effected by starting zone characteristics, climate, latitude, vegetation patterns, ground roughness and path confinement (particularly in the track and runout zone).

Mears (1992) suggested calculating the **magnitude-probability** (see Nomenclature) relationship for an area in order to understand the consequences of improper land use. To be able to make such designations, **hazard zone analyses** (see Nomenclature) must be carried out. This can be done by **observational** or **analytical** methods to estimate avalanche motion.

In British Columbia work is underway to establish **Environmentally Sensitive Areas** (ESA's), particularly with respect to avalanches. An area is sensitive if timber harvesting may cause snow avalanches that could destroy man-made structures or valuable natural resources. Although most of the risk is associated with small avalanches, it is important to recognise long-return period paths. To be able to assess areas for hazard designation, an understanding of the frequency and magnitude of avalanches, and their relation to terrain variables within that region, is essential. Of particular interest are the lateral or longitudinal extension of snow avalanche paths, increases in the number of snow avalanche trigger zones, and increases in the magnitude and frequency of avalanches.

1.4 CONCLUSIONS

Avalanche research has been primarily concerned with the mechanics, prediction and management of natural snow avalanches. However early avalanche research (Allix, 1924) suggested an increase in avalanche frequency (and the appearance in otherwise safe areas) of avalanches as a direct result of human interference. This pioneer work was never carried any further.

High-risk, high-frequency avalanches are now being recognised as vital to the management of risk within avalanche regions and are beginning to receive more attention. The implications of such work are to allow a better understanding of these processes and so promote the safe recreational use and development of mountainous regions. In addition, the implications of modifying the terrain, particularly the vegetation cover, will foster a responsible attitude to land management.

The following chapter provides a detailed review of the prediction of extreme (low-frequency) runout of avalanches. This will focus on both physical modelling (which is applicable to both low- and high-frequency avalanches) and statistical modelling. The latter approach is being utilised in my study of high-frequency sites and so an understanding of this methodology is important. This chapter also indicates how these approaches are incorporated into land management studies.

Chapter 3 presents a review of work on avalanche frequency and the use of statistical models in hazard zoning and also discusses the effect of climate on avalanche frequency. Chapter 4 describes field work and photo interpretation of high-frequency paths, with a statistical description and comparison with low-frequency paths. I then go onto develop statistical models to estimate high-frequency avalanche runout. Chapter 5 describes work on distribution-fitting to frequency data from Rogers' Pass and subsequent correlation of frequency with terrain. Finally, Chapter 6 provides an overview of this thesis with final conclusions.

2. PREDICTION OF EXTREME RUNOUT

2.1 INTRODUCTION

The prediction of extreme runout of avalanches is a vital component of any hazard analysis and land-use planning exercise. If direct observation, path history, vegetation analysis or aerial photo interpretation are not possible (McClung and Schaerer, 1993), then numerical methods provide the only means of obtaining estimates. In Europe, where records of extreme avalanche events go back centuries, zoning of land into degrees of risk is common practise, but in North America it is necessary to use numerical methods.

The application of physical models, making full use of historical data, has been the traditional method of computing extreme runout for avalanche zoning, as well as providing further information on avalanche motion, such as velocity, to allow the calculation of impact pressure and so the design of defence structures. These methods have produced incorrect estimates (Frutiger, 1990) and so this problem led to the development of, simpler, statistical models. I will introduce the different types of physical and statistical models and describe how they have been applied. In the conclusions I will summarise the different models and comment on their usefulness and flexibility in avalanche zoning, as well as the ability of these models to help explain the motion of avalanches.

2.2 RUNOUT PREDICTION

2.2.1 Introduction

In this section I will briefly review the principle physical models used in avalanche hazard zoning and provide a comprehensive review of two different statistical methods that have been utilised in the prediction of extreme avalanche runout. These statistical models were first developed by Bovis and Mears (1976) and Lied and Bakkehøi (1980), and then

extended with the work of McClung and Lied (1987) and McClung and Mears (1991). Variations and applications of these two basic themes will also be discussed.

2.2.2 Physical Models

Several physical models have been developed and are able, to varying degrees of accuracy, to compute velocity, runout, flow depth, deposit depth and lateral extent. These types of models require input in the form of terrain parameters and material properties. The terrain variables can be measured in the field; however certain assumptions need to be made about material properties, particularly friction coefficients. These have not been measured (although they have been back-calculated) and there is a high degree of uncertainty in their use.

There are two main physical models; these are the Swiss Model (Salm *et al*, 1979) and the Perla-Cheng-McClung (PCM) Model (Perla *et al*, 1980), both of which are extensions of Voellmy's (1955) original physical model. More complex models exist (Norem *et al*, 1989); however they are plagued by a need to make further assumptions.

Original work on physical models was produced by Voellmy (1955), later summarised by Sommerhalder (1965). Avalanche flow was modelled as a point mass, from which a simple force-momentum relationship with driving and resisting forces was derived. Within the resisting forces, two constants, drag (ξ) and dynamic friction (μ) were used. Velocity, runout (from a reference point) and flow height could then be derived. Both of the above coefficients $\{\xi, \mu\}$ are crucial to runout and cannot be determined to great precision. Experience in using the model is necessary in order to pick combinations of $\{\xi, \mu\}$ that fit known or likely values (Buser and Frutiger, 1980). On a slope of known runout, different pairs of $\{\xi, \mu\}$ can be calculated to fit a given runout distance (ie solutions converge on that point) and so accurate estimates of velocity and impact pressures, in the runout zone, can be achieved (McClung, 1990).

The Swiss model is a refined version of the original Voellmy (1955) and Sommerhalder (1965) methods. The model divides the slope into starting-zone, track and runout-zone of constant slope and then "marches" a calculation of velocity downslope. This model was specifically calibrated for use in Switzerland and so, unless detailed records are available, systematic error can occur if this model is applied to other regions.

The PCM model also uses a force-momentum relationship and, like the Swiss model, "marches" a calculation of velocity downslope. However, the PCM model uses a detailed terrain profile, typically with segments of constant slope, when "marching" the calculation of velocity downslope.

2.2.3 Bovis and Mears (1976)

In 1976 Bovis and Mears published a study on the prediction of snow avalanche runout from terrain variables using a least-squares regression equation. Their data consisted of track gradient (X_1), runout zone gradient (X_2) and starting zone area (X_3) for 67 avalanche paths from Colorado. X_2 and X_3 are both sine functions of the slope angle in degrees. Paths involving impact on the adverse slope were not used.

They found that X_1 was highly correlated with runout distance, while X_2 and X_3 were negatively correlated with runout (a lower runout angle means a longer runout). The best regression equation was with X_1 and yielded

$$Y = 213.7 + 11.4X_1$$

with an r^2 of 0.65 (where r is the correlation coefficient).

Bovis and Mears went on to suggest that further terrain parameters (which describe path configuration and account for regional differences) would increase the accuracy of the approach. They also hinted at the possibility of regional differences between avalanche terrain variables and avalanche runout.

2.2.4 Lied and Bakkehøi (1980)

Lied and Bakkehøi gathered data on 10 terrain parameters (3 categorical) from topographic maps, aerial photographs and ground surveying for 111 low-frequency avalanche paths in Western Norway. Figure 2.1 shows geometrical variables used in this, and other studies. Of these, the most important is angle β , the point where the slope angle first declines to 10° proceeding downslope from the starting zone. This " β -point" was picked as a reference position from which runout distance could be assessed. The angle from the top of the starting zone to the outer end of the avalanche debris is represented by angle α . From this angle, extreme runout is easily calculated.

From their least-squares regression, the only significant predictor was β with a regression equation of the form

$$\alpha^\circ = 0.98\beta - 1.2^\circ$$

with an r^2 of 0.93 and an SD (standard deviation of the residuals) of 2.44° . With the use of 4 predictor variables a marginally better regression equation was attained.

In 1983 Bakkehøi *et al* extended the above analysis by increasing the number of paths in the database from 111 to 206 and adding several new predictor variables. Again, the only significant predictor was β giving the following equation

$$\alpha^\circ = 0.96\beta - 1.4^\circ$$

with an $r^2=0.92$ and an $SD=2.3^\circ$.

Figure 2.1 Geometry variables of an avalanche path used in extreme-runout analyses (Nixon and McClung, 1993).

Figure 2.2 Runout ratio fitted to extreme value probability distribution for five mountain ranges. (\diamond) Sierra Nevada, (\times) Colorado Rockies, (+) coastal Alaska, (Δ) Canadian Rockies, (\square) western Norway (McClung and Mears, 1991).

Their results also suggested that steep paths attain a relatively short runout, while there was no statistical tendency for confined paths to have greater runout. In 1989 Lied and Toppe added parameters measured from Digital Terrain Models, however results again indicated the dominance of β as a predictor.

2.2.5 McClung and Lied (1987)

McClung and Lied (1987) performed a multiple regression analysis using a dataset of 212 avalanche paths from Western Norway. The single best predictor variable was again angle β , while other predictor variables were not significant in a multiple regression model.

McClung and Lied introduced two dimensionless scaling parameters whereby runout is estimated from the β -point to the α -point. These were

$$\frac{\Delta X}{X_{\beta}}$$

$$\frac{\Delta X}{H_{\beta}}$$

where ΔX is the horizontal distance between α and β , X_{β} is the horizontal distance from the β -point to the start of the path and H_{β} is the vertical distance from the β -point to the top of starting zone. A least squares multiple regression was performed on each dimensionless parameter against the predictor variables. The correlation coefficients were close to zero, suggesting they were statistically independent of all the predictor variables. The assumption of statistical independence was found to be better for the former dimensionless parameter and so was this was used in the following analysis, being termed the **runout ratio**. They found that the parameter followed an extreme value (Gumbel) distribution. The 50 highest values of $\Delta X/X_{\beta}$ were plotted against the reduced variate (ie plotted on Gumbel probability paper), defined as $-\ln[-\ln(P)]$, where Weibull plotting positions were used, and then a regression analysis was performed on the data to see how well the distribution fitted. This gave an

$r^2=0.99$ and a standard error $S=0.0064$. This then gives the model

$$\left(\frac{\Delta X}{X_\beta}\right)_P = 0.1419 - 0.07978 \ln[-\ln(P/100)]$$

where $0.5 \leq P < 1.0$. This states that $100 \times P\%$ of avalanche paths in the data set have a horizontal reach less than $(\Delta X/X_\beta)_P$ (where P is the non-exceedance probability). The use of P is determined by the user in an estimate of the level of acceptable risk.

This work was extended in 1991 (McClung and Mears) by comparing 526 avalanche paths from five mountain ranges, consisting of free running 100 year avalanches. Two of the ranges were continental and three maritime. Data from each mountain range was shown to obey a Gumbel distribution. Their results (Figure 2.2) showed that regional climate did not exert an influence over runout for low-frequency avalanche events, as regression lines for continental and maritime climates were inter-mixed.

2.3 AVALANCHE ZONING

2.3.1 Avalanche Zoning Schemes

Avalanche zoning is the process of delimiting mapped avalanche boundaries and the application of restrictions to land use within these avalanche areas. The statistical and physical models described in this chapter are the primary models used in delimiting avalanche boundaries. This section will briefly introduce the different zoning schemes in use and describe the procedure for avalanche zoning using physical and statistical models.

The Swiss method of avalanche zoning is based upon four categories, with increasing avalanche frequency and impact pressures in higher risk zones. The **Red** zone, is a high risk, high-frequency, avalanche area; all development is usually restricted and current buildings are required to have protection. The second, or **Blue** zone, allows new residences provided they

are protected against impact. Structures that attract large numbers of people are not permitted (eg schools). The third, or **Yellow** zone, is thought to be affected by air blast from extreme avalanches. The final, **White**, zone is a low hazard zone.

In Canada, an avalanche **hazard line** has been established in most areas (Freer and Schaerer, 1980). This marks the limit of large infrequent avalanches; land within this line has development restrictions. In certain situations the Swiss system may be necessary, and so, could be applied once detailed data are available.

2.3.2 Use of Statistical and Physical Models

The physical and statistical models reviewed in the previous sections, demonstrate the dichotomy existing between the estimation of extreme avalanche runout. Physical models have proved difficult to apply as they require the estimation of $\{\xi, \mu\}$ and extensive field testing. Bakkehoi *et al* (1981) stated that it would be difficult to predict avalanche runout to $\sim 10^2$ m accuracy for a $\sim 10^3$ m length path. Calculations of velocity, flow depth, impact pressure and lateral spreading are similarly limited. Frutiger (1980) provided an example of field calibration of the Swiss model. He originally zoned the Galena Basin in the Central Sierra Nevada, identifying 49 avalanche paths. Two years later a severe storm caused 16 of these paths to avalanche, 6 of them beyond the zoned region. Frutiger then used these results to calibrate the friction coefficients in his model. This is fortuitous as it allowed refinement of the zone boundaries; however it could have proved disastrous if further development had taken place since his original study.

Statistical models arose out of a need for greater accuracy in calculating extreme runout distance. Regression models are a very simple method of study and have proved satisfactory for avalanche zoning. The application of the extreme-value model (Gumbel distribution) to runout ratio data has also proved successful and can predict extreme runout to a greater accuracy than the previous regression equations. It also has the benefit of being

able to easily define the level of acceptable risk appropriate to the situation. McClung and Mears (1991) showed that different regions have different coefficients for this distribution. This requires the collection of terrain parameters for a new region before this method can be used for avalanche.

McClung (1985) combined the best features of both the physical and statistical models into a new model, which he later refined (McClung, 1990). This comprises the determination of avalanche runout from direct observations or by empirical calculations if direct observations are not available. Once completed, this runout distance can be used in physical models to calculate velocity and impact pressure, as well as other flow characteristics used in avalanche-zoning. Physical models require the use of unknown parameter values $\{\xi, \mu\}$. As the runout position has been measured or estimated, estimates of avalanche velocity can be scaled as values for $\{\xi, \mu\}$ must converge to 0 at the extreme runout position. This allows accurate estimates of velocity in the runout zone, and so may be used for the design of avalanche defence structures.

For avalanche zoning to be effective, a database of extreme runout distances needs to be collated if the terrain models are to be used. The extreme-value distribution of the runout ratio can then be used to estimate runout of the limit avalanche if field evidence is not available. This information can be used to delimit the Blue zone and calculate velocity and impact pressure with a physical model. If the PCM model is used to calculate velocity, terrain profiles are necessary to segment the path. Impact pressures can be used to delimit the red zone, as well as aid in the design of buildings or defence structures in the runout zone.

2.3.3 Conclusion

In conclusion, physical models of avalanche motion are unable to provide accurate estimates of extreme avalanche runout. As a result, statistical methods have been developed

to estimate runout. Lied and Bakkehøi (1980) showed that angle β was the single most important predictor of angle α . McClung and Lied (1987) went onto show that the runout ratio followed a Gumbel distribution.

McClung (1990) went on to develop a two-stage procedure for avalanche zoning. This involves the calculation of the extreme runout. This information is then used in physical models to provide better estimates of velocity, and other flow parameters, in the runout zone.

Avalanche zoning is an important feature of the mountain environment as increased encroachment in potentially dangerous regions take place. Consequently, many countries now enforce avalanche zoning as one method of avalanche hazard mitigation. The above two-stage procedure allows avalanche zoning to be performed and can lead to the development of defence structures through the calculation of impact pressures, runout and lateral spreading.

3. AVALANCHE MAGNITUDE AND FREQUENCY

3.1 INTRODUCTION

Studies of the magnitude and frequency of events are common in many natural hazard management programs to design defence structures for given event magnitudes. Flood studies were the first to develop statistical relations between flood volume and flood frequency and more recently, avalanche studies have used historical data for similar purposes. In this chapter I will summarise distribution fitting to records of avalanche magnitude and frequency. Chapter 5 will use techniques similar to those applied in the work reviewed here, however I am able to analyse an extensive dataset of 43 avalanche paths with 24 years of avalanche occurrence records. If avalanche frequency can be assumed to follow a certain probability distribution, then this information can be used in avalanche risk mapping. I then discuss the interactions of micro-climate and terrain. As climate and terrain interact to produce the record of avalanche frequency observed, any study is incomplete without a description of these two factors.

The magnitude and frequency of an avalanche on a single path depends upon the position along the path from which observations are made. Generally, the frequency increases and the magnitude decreases (and vice versa) the further from the runout zone that observations are made. Some reference point for avalanche motion is required. In the case of Fitzharris (1981), for example, events were only recorded if the railway line at Rogers' Pass was crossed by an avalanche.

If a probability distribution can be associated with avalanche frequency, then this can be used to define frequency in calculations of risk. Similarly, if a probability distribution can be associated with avalanche magnitude, then this information can be used to design defence structures for a given magnitude event. Section 1.1 introduced the following probabilistic

definition of risk

$$P_s = P_h \times P_e \times P_v$$

where P_s is specific risk, P_h is avalanche frequency, P_e is exposure (fraction of time or space an object is exposed to the hazardous events) and P_v is vulnerability (the fraction of damage expected from an event of a given size). P_e is approximately independent of magnitude, while P_v is related to the magnitude of the event and the fragility of the threatened object. P_h is the probability for all events which reach or exceed a given location and is defined as the **exceedance probability**, or $1/T$, where T is the return period of events of a given magnitude or greater. Exceedance probability is calculated from a probability density function or probability mass function derived from assumptions and data about the event frequency. If the frequency of events is assumed to follow a certain distribution, this may be used to calculate P_v .

3.2 AVALANCHE MAGNITUDE AND FREQUENCY

3.2.1 Fitzharris (1977)

Fitzharris (1977) obtained records of avalanche magnitude and frequency for Rogers' Pass, British Columbia, for the period 1909-1977. Avalanche events were recorded with respect to the railway, and were low-frequency as the railway is located at the end of the runout zone. Fitzharris then performed chi-square goodness-of-fit tests, and visual inspection, in order to determine the best probability distribution to fit to avalanche magnitude and frequency. The Gamma distribution seemed the most appropriate distribution to describe avalanche frequency, while avalanche magnitude (mass) fitted the Jenkinson fitted Gumbel distribution.

3.2.2 Föhn (1975)

Föhn (1975) showed that avalanche frequency, for an unforested avalanche path, obeyed a Poisson distribution. The occurrence data were recorded with respect to a road located at the end of the runout zone. As with Fitzharris, the avalanche path was low-frequency. Föhn (1979) later used this result to calculate the encounter probability, using this information in a risk analysis. Föhn (1981) also showed that avalanche magnitude followed a Gumbel distribution. This, he suggested, could be used for zoning areas with respect to different return periods.

3.3 CLIMATE AND AVALANCHE FREQUENCY

Regional climate is the predominant effect on regional avalanche frequency, as the effect of different weather systems on avalanching is often distinct. However, the complex interactions between micro-climate and terrain, at a local scale, controls the frequency of avalanching on individual avalanche paths. Very little work, other than case studies, has been produced on the effects of micro-climate on avalanche frequency. Chapter 5 presents an analysis of avalanche frequency with respect to terrain and climate variables. If avalanche path frequency is predominantly controlled by terrain variables, then it would be possible to predict frequency from easily measurable terrain parameters. This information could then be used to define frequency (P_h) in risk analyses.

Separating the effects of terrain and climate is very difficult as they are so closely linked. For example, elevation is a terrain variable, however the effects of changes in elevation on avalanche frequency are primarily due to changes in snow fall supply. A further example of this complex relationship is demonstrated by Bakkehöi (1987). He showed that the 3-day sum of precipitation, immediately preceding an avalanche event (when plotted on normal probability paper), followed a normal distribution. However regressions lines for each

of the 5 paths he studied, varied considerably. He suggested that these variations were primarily due to differences in terrain.

3.4 CONCLUSIONS

The collation of avalanche occurrence data is a long, complicated, process, only possible in areas with long-term records. Very few areas meet this criteria and therefore analyses are few. With such long data sets there are several sources for error; however the potential benefits in using these data, with respect to avalanche zoning, are many. Results of distribution fitting so far suggest that avalanche magnitude follow a Gumbel distribution. This information has been used to zone specific areas with respect to runout for different return periods and in the design of defence structures for certain magnitude events. Avalanche frequency has been shown to follow a Poisson distribution. This result can then be entered into calculations of risk as P_h , by estimating the encounter probability.

This chapter has also highlighted the intricate links between climate and terrain with respect to avalanche frequency. Any study of avalanche frequency and terrain must attempt to account for micro-climate. Chapter 5 will analyse avalanche frequency at Rogers' Pass, British Columbia, with respect to climate and terrain.

4. TERRAIN ANALYSIS

4.1 INTRODUCTION

In this chapter I provides an analysis of high-frequency avalanche path terrain, with particular emphasis on runout. This work uses similar methods employed by Lied and Bakkehøi (1980) and McClung and Mears (1991) to analyse avalanche paths and so provide a method of predicting avalanche runout from terrain parameters. This prediction can be used directly in a zoning policy or can be used as input in a physical model of avalanche motion and so provide estimates of avalanche velocity and impact pressure in the runout zone (see Chapter 2 for a fuller description of these methods). So far work has only provided this information for low-frequency avalanche paths; however, as Chapter 1 demonstrated, it is frequency that controls risk. An increase in frequency increases the risk and so knowledge of the characteristics of high-frequency avalanche paths, particularly their runout, is essential.

Extensive field work was aimed at collating a database of terrain features from avalanche paths in the Coast Mountains and Columbia Mountains of British Columbia and the Canadian Rockies. Section 4.2 deals with the criteria used to select avalanche paths and the use of air photos to collect further terrain parameters. Field techniques are discussed next, and descriptive statistics of the final data set are provided and compared to those of other low-frequency avalanche sites. A regression analysis is performed on the data set, with particular emphasis on estimating avalanche runout for land-use planning. The method is then compared to results obtained from an extreme-value model (see §2.25 for a detailed summary of this method).

4.2 DESCRIPTION OF METHODS

4.2.1 Selection Criteria

Four criteria were used to select avalanche paths at high-frequency sites:

- (1) High Event Frequency - a minimum frequency of once in 15 years was used. The return period could only be estimated for those paths on which avalanche activity had been monitored. For this reason, paths affecting highways were used, nearly all of which come under the jurisdiction of the Avalanche Section at the Ministry of Transportation and Highways. Computerized databases were available of all avalanche occurrences along each highway since monitoring began. In comparison, previous studies have focussed on low-frequency sites whose return period ranged from 50 to 300 years.
- (2) Delimited Runout - trees need to be present in order for the runout terminus to be located.
- (3) Unobstructed Runout - paths were not selected if there was an obstructed runout (ie they ran up the adverse slope).
- (4) Simple Starting Zones - multiple gullies and/or multiple starting zones were avoided as these can complicate avalanching, often leading to multiple avalanche events.

4.2.2 Measurement Procedures

Paths were selected initially from avalanche atlases of the monitored regions and were later field checked. Once paths were selected, their α -point was located and the α -angle measured using a Suunto clinometer to an accuracy of $\pm 0.5^\circ$. Each path was then traversed to the β -point and the β -angle measured, followed by the δ -angle. A foresters' measuring line was used to measure the slope distance between α and β , which was later converted to ΔX (see Figure 2.1 for definition of terrain parameters).

4.2.3 Problems Encountered

While field work was performed several general trends were apparent, as well as several unforeseen problems. These were:

(1) Paths with Large Vertical Drops - these tended to have multiple gully starting zones and so were a poor choice in view of the restrictions noted in the previous section. In their study of low-frequency paths, McClung *et al* (1993) noticed a vertical scale-effect, and so restricted their study to paths with a vertical range of 350-1100m. Nixon and McClung (1993) noticed a length scale-effect and went on to partition data for the purpose of avalanche zoning. Although no length or vertical scale effects were apparent in this study, it was generally noted that large paths with multiple gullies had long return periods.

(2) In order to assess the frequency of events on avalanche paths, avalanche occurrence data were acquired from the Ministry of Transportation and Highways. These records cover a period of 15-40 years, depending on the highway in question. Several regions have records complicated by the use of hazard mitigation measures. At Kootenay Pass for example, prior to the use of explosives as a control measure (1975), the average number of avalanches reaching the highway each year was 48. However since the use of explosives, the annual average has increased to 101. Other measures such as catchment benches, mounds or deflectors may reduce the frequency of events reaching the highway. However, the majority of areas maintained by the Ministry simply employ road closures, combined with explosive control, during high risk periods. In some cases (Eg Sheep Creek) the highway dissected the upper part of the path (creating a very effective catchment bench). Accurate records of full running avalanches are probably poor.

(3) Many paths, particularly those at Kootenay Pass, were noted to be short and steep, often of the "hockey stick" type. "Hockey stick" avalanche paths, so named for their appearance in profile, have a short, steep track, with a rapid transition to a low gradient runout zone.

(4) In 10 out of the 46 paths, the β -point was located **below** the extreme runout (some paths had β and α at the same location, and therefore $\delta=0^\circ$). In several cases, a β -point was not measurable (ie a steep gorge in which the path ended before the bottom). The β -point may be more a function of other processes (eg hydrological), having very little relevance to the location of the end of the path. It is likely that the high correlation of the angle β to the angle α (see §2.24) is simply a function of the relative closeness of these two points. Lied and Bakkehøi (1980) defined several different arbitrary positions along the avalanche path in order to measure extreme runout. They eventually selected 10° as the local slope angle for the value of β , suggesting that it corresponded to the lowest dynamic friction coefficient used in physical models. Therefore it is at this point that avalanches begin to decelerate.

A greater β -point angle would be a possible solution and has already been applied by McKittrick and Brown (1993). However, field measurement error is increased (due to effect of slope foreshortening) by the use of a greater value.

(5) In many cases paths failed to reach the highway and so were noted as "potential." The accuracy of records of avalanche occurrence for these paths is unknown.

(6) Many areas were logged before, and since, the atlases were produced. This prevented the use of many paths. Some areas had been burned or logged at the turn of the century, but were used as long as the maximum runout could be located.

(7) Many paths were on the opposite slope to the road and therefore crossed the river and moved up the adverse slope before coming to a stop. Where they ran onto the valley floor they could not be surveyed as the β -point was inaccessible.

(8) Many large paths ran out onto alluvial fans and caused a confused record of mixed events (debris flows and avalanches). This was further complicated by wet and dry snow avalanches which may take divergent runout trajectories.

(9) Cutslopes (man-made cuttings) were avoided as they represented man-made avalanche

slopes. It was noted that the Revelstoke-Mica region had a large number of high-frequency cut slope avalanche paths. These may represent an interesting data set with respect to high-frequency avalanching. Ironically the development of a road may actually create avalanche problems.

Conversely, embankments (particularly in the runout zone) create steeper runout zones, while the road itself may well act as a catchment bench (particularly on steep slopes which appear to produce low volume avalanches). Many of the steep areas (with high-frequency avalanches) with the road in the track or runout zone had the avalanches ending at the road because of this catchment bench effect.

4.2.4 Air Photo Interpretation and Digitizing

Once suitable avalanche paths were selected and field checked, with measurements of ΔX , α , β and δ taken, further terrain parameters were collected from air photos. Bakkehoi *et al* (1983) collected terrain parameters from 1:50,000 topographic maps, providing a locational accuracy of $\pm 50\text{m}$. The accuracy of their data was also limited by uncertainty introduced in the location of the avalanche paths on the map. For these reasons, further terrain parameters were collected in the present study using aerial photography and the Carto Instruments AP190 analytical plotter. Using UTM coordinates, the stereo models were linked to topographic maps to yield absolute units. Information was then digitized from the air photos.

To create a corrected stereo model of the air photo stereo pairs, a two step procedure comprising **relative orientation** and **absolute orientation** is performed by the operator. Relative orientation removes the combined y-parallax error, through an iterative process, created by radial and relief displacement over the stereo pair. Absolute orientation locates UTM coordinates (control points) within the stereo model. If available, surveyed data or

large-scale maps should be used; however only 1:50,000 topographic maps were available for the avalanche paths in this study. Positional error on the topographic maps is about 50m in the x, y and z directions, where x and y are location axes oriented N-S and E-W and z is elevation. Positional error between the control points and the stereo model was less than 20m in the x and y directions and less than 10m in the z direction. For Kootenay Pass, 1:5,000 mapping was available, yielding location errors to less than 5m in the x and y directions and approximately 1m in the z direction.

It was decided to work with medium to large scale photos; however it was soon discovered that photos of scale 1:10,000 and larger had too much parallax and were too difficult to work with. For this reason, 1:20,000 scale photography was found to be more suitable, although a range of photography from 1:15,000 to 1:40,000 was eventually used (see Appendix 2 for a list of avalanche paths included in this study and the aerial photography used). Photography at a scale of 1:40,000 allowed better absolute orientation, as the smaller scale provided more anthropogenic information; however the digitizing process was more difficult.

Once relative and absolute orientation was complete, the terrain parameters were digitized from the stereo model. The following parameters were measured, or calculated from measurements, from the stereo model: average track angle, area (total area of the avalanche path), catchment area (maximum area that unstable snow can release from), track width (measured across the central portion of the track), runout zone width (measured at the extreme runout), vertical drop, average slope angle (α), path length (straight line from path centre line at the top to path centre line at the bottom), and track confinement (categorical). Track confinement was broadly characterised as

(1) Confined - a gully.

(2) Intermediate - shallow gully.

(3) Unconfined - open slope.

4.2.5 Curve Fitting

One of the most notable characteristics of the database of high-frequency avalanche paths is the nearness of the α -point to the β -point (see §4.3.1) and, consequently, the small value of ΔX . In fact 10 of the 46 paths have $-\Delta X$ values (Figure 4.1 shows a frequency histogram of ΔX values). There is an element of uncertainty in measuring ΔX on these paths (see earlier discussion), and indeed, 5 were unmeasurable as the valley simply dropped into a river before the 10° slope angle was reached. This produced missing values in the database and lack of confidence in some values that are present. However, since the β -point is significantly related to runout (see §4.3.2), it is important that these paths be included in the database.

Initially these 10 paths had their centre line digitized on the AP190. The raw data were then transformed so that they could be plotted on an x-y graph (Figures 4.2A and 4.2B are examples of avalanche path profiles). All paths were subsequently plotted on x-y graphs in order to assess the quality of the ΔX estimation. Once plotted, a least squares regression model of the form $y=a+bx+cx^2$ was fitted to each avalanche path. Regression fits were very good with r^2 values greater than 0.990; in only 2 of the models was the x^2 term not significant. Visual inspection of the fitted curves highlighted the steep and straight profiles of the paths. In fact, linear regression models of the form $y=a+bx$ attained r^2 values of 0.94. Consequently fitted regression models were very straight causing estimates of ΔX to be very large (see Table 4.1). This error is unacceptable; however it is caused, in part, by the limited accuracy of the digitization procedure. McClung and Lied (1987) noted similar problems.

Collinearity, due to dependence between the x and x^2 terms caused problems in fitting a second order polynomial. Although the x^2 term was significant, the regression procedure

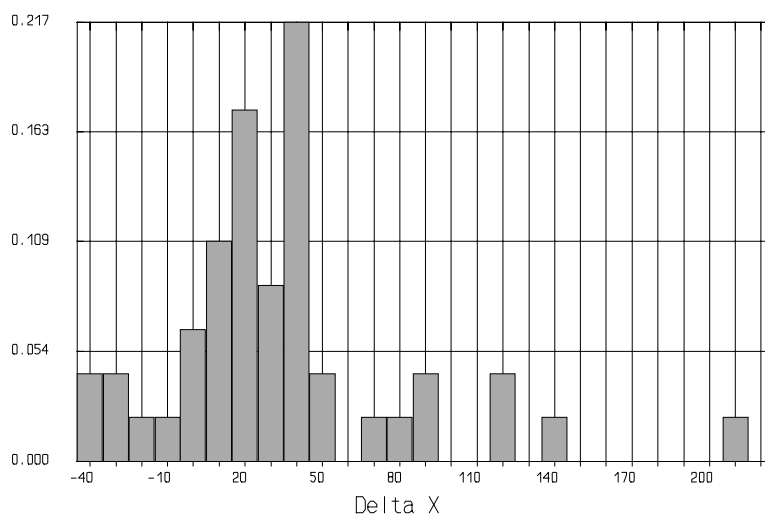


Figure 4.1 Frequency histogram for values of ΔX (units are in meters).

Path Number	Orthogonal Estimate	Regression Estimate	Field Measurement
TC55.7	-2218	-2538	-
BP44	-13	-28	-
BP42	-34	-378	-
KP20.2	-131	-235	-29
KP21.7	-268	-732	0
KP21.9	-2	-305	45
KP26.7	-649	-888	55
W0.9	-110	-286	30

Table 4.1 ΔX values from field measurements and regression estimates. The top half of the table contains paths $-\Delta X$ and the bottom half $+\Delta X$ values (units are in meters). Note the poor estimates of ΔX for both orthogonal and regression methods when compared to field measurements.

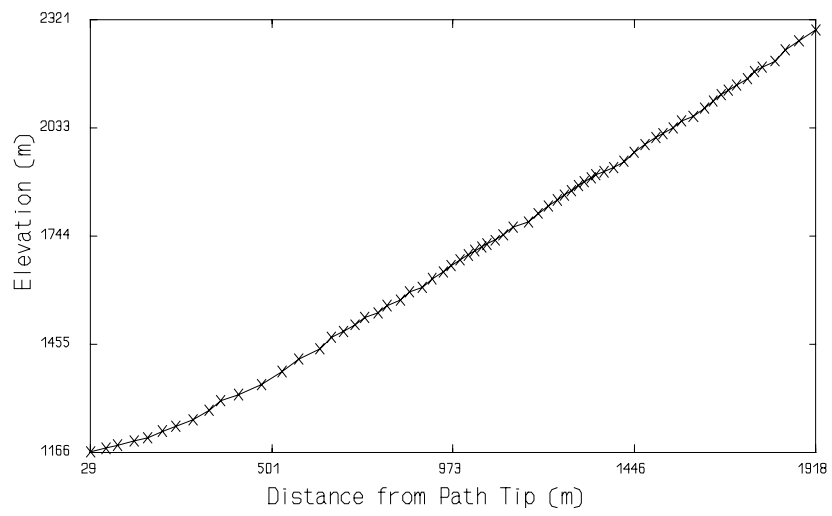


Figure 4.2A Example of digitized centre line plotted as a profile for Path 55.7 at Toby Creek

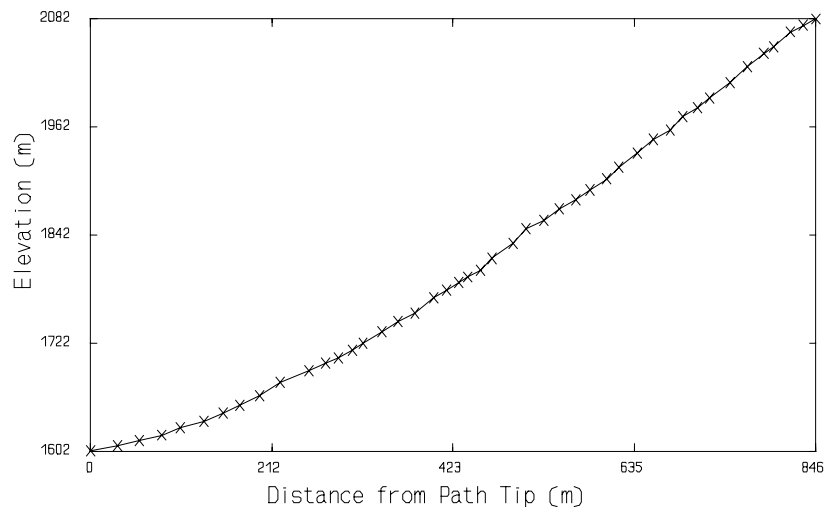


Figure 4.2B Example of digitized centre line plotted as a profile for Path 21.7 at Kootenay Pass

essentially fitted a straight line which provided a poor fit to the extreme runout where curvature of the path was apparent. It is essential to have a reasonable model fit in this range of the data, as typically this is where the β -point (which was to be estimated from the fit) occurs. Consequently, orthogonal polynomial coefficients were used to remove the dependence between the terms in the model. Again, two paths had the x^2 term insignificant and r^2 values for all fits were greater than 0.990. Visual inspection of the fits showed greater curvature in the lower extremities of the path. Estimates of ΔX were better than in the previous regression model, however they were still larger than those measured in the field. Table 4.1 shows measurements of ΔX compared with estimates from the two different regression models. It is noticeable that the orthogonal polynomial coefficients perform better; however the error is still unacceptable. As ΔX could not be reliably estimated, it was decided to abandon the method of curve fitting.

4.3 DATA ANALYSIS

4.3.1 Descriptive Statistics and Comparison with Past Results

Field work comprised field checking the selected avalanche paths throughout southern British Columbia (see Appendix 1 for a summary, and location map, of avalanche areas that were field checked). It was hoped that field measurements could be collected for the Coast Mountains and Canadian Rockies and Purcells. These data could then be compared with previous work in these two regions. However, the majority of monitored avalanche paths in British Columbia are in the Monashees, Selkirks and Purcells ($n=46$), collectively known as the Columbia Mountains. For this reason, very few data points were collected in the Coast Mountains ($n=9$) and Canadian Rockies ($n=16$). Consequently, there were too few data points to perform statistical analyses on. The Columbia Mountains form a natural biogeoclimatic and physiographic region (Young, 1985); in this thesis these paths have been merged to form

one data set.

Table 4.1 shows descriptive statistics for the Columbia Mountains avalanche paths. Appendix 3 contains descriptive statistics of terrain parameters from low-frequency paths in the Canadian Rockies and Purcells, western Norway, Coastal Alaska, Colorado Rockies, Sierra Nevada, British Columbia Coast Mountains and south west Montana.

In comparison with these mountain ranges, there are some distinctive characteristics exhibited by this set of high-frequency paths. Most notable is the much higher mean value of α (33.3°); western Norway has the highest value of α in the low-frequency data sets, at 29.4° , while the Sierra Nevada has the lowest at 20.1° . There is also a very small range of α values. Therefore, these high-frequency paths are significantly steeper than their lower frequency counterparts.

Also distinctive is the small difference between α and β . The maximum value of β is no larger than those found in the low-frequency data, although it is comparable with western Norway which has the steepest paths in the low-frequency dataset (note that this value does not include all paths, as some had unmeasurable β values). Mean values of β in the low-frequency data sets ranged from 26.3° to 32.6° . Since α and β are similar in value, ΔX is short and the runout ratio is small. The mean value of ΔX is 29m, while the low-frequency data ranged from 66m to 354m. However, as X_β was comparable with the low-frequency data sets the runout ratio was low (mean of 0.064). This should be compared with the low-frequency data sets, where the runout ratio ranged in value from 0.11 to 0.49. This demonstrates that the steeper the path, the lower than runout ratio. The runout ratio also exhibited a fairly large range, a result of several outliers at both the upper (noticeably from Rogers' Pass), and lower tails.

Values of δ are higher than those found in the low-frequency data sets, suggesting a steep runout with the path terminus at or around the β -point. There was a large range in

Parameter		Columbia Mountains (n=46)
$\alpha(^{\circ})$	min	25.2
	med	32.5
	avg	33.3
	max	41.5
	std	4.0
$\beta(^{\circ})$	min	27.0
	med	33.0
	avg	34.2
	max	46.0
	std	4.0
$\delta(^{\circ})$	min	0
	med	6
	avg	7.9
	max	25
	std	7.1
H(m)	min	125
	med	471
	avg	538
	max	1260
	std	303
$\Delta x(m)$	min	-40
	med	29
	avg	38
	max	217
	std	49
$\Delta x/X_{\beta}$	min	-0.102
	med	0.044
	avg	0.064
	max	0.382
	std	0.099

Table 4.2 Descriptive statistics of parameters for the Columbia Mountains.

vertical drop (H); however the mean is fairly low and is comparable with that of the Sierra Nevada and the Colorado Rockies.

4.3.2 Regression Models

Using data collected from the stereo models, a least squares regression model was created, following the methods of Lied and Bakkehoi (1980, see §2.24). Descriptive statistics on the 12 terrain variables are given in Table 4.3. First, a Pearson product-moment correlation matrix was compiled for the 11 predictor variables against α . Significant inter-correlation with α are given below:

	r-values
Track Angle	0.64
Catchment Area	-0.41
Area	-0.36
Aspect	-0.36
β	0.77
H_β	-0.46
X_β	-0.56

Track confinement (0.25) was also an important single variable correlation. A multiple regression was then performed on the above 8 predictor variables; however the only significant variable in this analysis was β . A simple regression using this term gave the model

$$\alpha = 9.56 + 0.69\beta$$

with an r^2 of 0.59 and a standard error (SE) of 2.30. Figure 4.3 shows a plot of α against β .

An alternative regression model, estimating the horizontal length (L) of the avalanche path, was also explored. In this analysis track angle (-0.60), catchment area (0.77), area (0.79), track confinement (-0.55), β (-0.55), H_β (0.98) and X_β (0.99) were all significantly correlated with L. A stepwise multiple regression was then performed on the above 7

Variable	Mean	SD	Min	Max
Track Angle ($^{\circ}$, TA)	33.9	5.2	22.1	44.2
Catchment Area (ha, CA)	8.5	14.9	0.4	81.4
Track Width (m, TW)	117	109	16	622
Runout Zone Width (m, RZW)	125	113	22	620
Area (ha, A)	15.8	20.8	0.7	108.0
Aspect* (AS)	8.1	1.7	4	13
Track Confinement* (TC)	1.9	0.9	1	3
β ($^{\circ}$)	34.2	4.0	27	46
δ ($^{\circ}$)	7.9	7.1	0	25
H_{β} (m)	520	283	127	1329
X_{β} (m)	802	499	152	2212
α ($^{\circ}$)	33.3	3.9	25.2	41.5

Table 4.3 Descriptive statistics of the terrain variables used in the regression analysis. See text for definition of categorical variables denoted by (*).

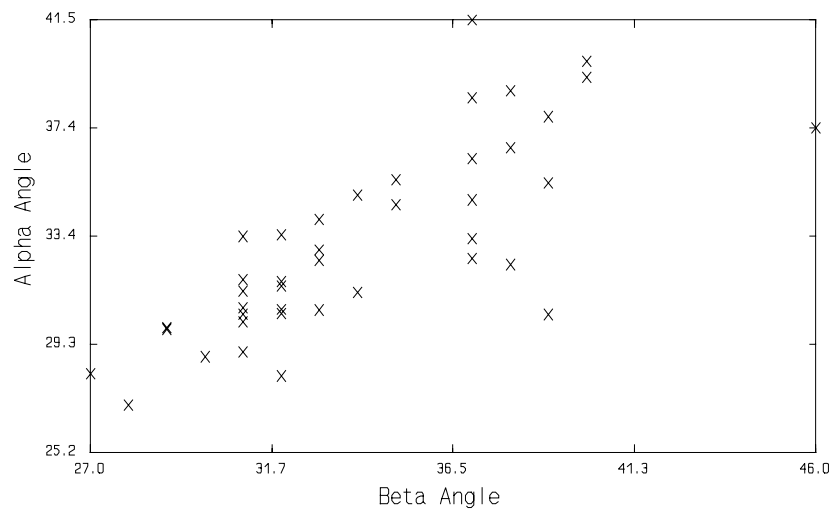


Figure 4.3 Plot of α against β

predictor variables, giving a model of the form:

$$L = -92.2 + 3.06TA + 1.03X_{\beta}$$

with an r^2 of 0.99 and a SE of 39.7. This model is able to provide significantly better estimates of avalanche runout than the above single variable model estimating α and is therefore recommended. Two further regression models were fitted to the data using predictor variables that do not require the location of the β -point; however low r^2 values and high SE values made these models unsuitable for avalanche zoning.

As with previous work, β is the only significant variable for estimating α . However this has limited practical application because of the large number of paths with $-\Delta X$ values and therefore uncertain or unknown β -points. Regression models using variables that do not require the location of the β -point provide poor fits to the data. Single variable correlations confirm that as α increases, β and track angle increase, while X_{β} , H_{β} , area and catchment area decrease. Aspect was negatively correlated with α . This may be coincidental as the frequency histogram (Figure 4.4) shows a distinct clustering around southerly aspects, likely a product of the east-west routing of most highways in British Columbia. Although this could lead to northerly aspects, many highways are south facing because of engineering and geologic factors. An alternative regression model, using predictor variables to estimate L, provided a better fit to the data.

In the following section I demonstrate that the extreme-value model can be used with these data to estimate avalanche extreme-runout. As the correlation between α and β is not strong, this latter method will provide better estimates of extreme-runout.

4.3.3 Extreme-Value Models

Following the method of McClung and Mears (1991), an extreme-value model was used to analyse the runout ratio. As both length and angle measurements were taken in the

field (and from air photos) it was possible to compare results from calculating the runout ratio using these two methods. The length method yielded a mean of 0.064 and an SD of 0.099, while the angle method yielded a mean of 0.051 and an SD of 0.129 for the data set. The data are slightly different for the following reasons:

(1) Measurement errors are multiplied through the analysis. Several paths had starting zones difficult to view from both the α and, particularly, the β -point, due to heavy vegetation. In some cases δ values were difficult to measure because of heavy vegetation; in addition, the measurement of this angle was adversely effected by the closeness of α and β , causing significant over-estimation. In the calculation of the runout ratios, this tends to produce over-estimates.

(2) It was noted that certain paths with small ΔX distances had α and β angles the same. This then records a runout ratio of 0 by the angle method and does not indicate the true runout ratio, indicating the limited accuracy of the clinometer in such situations.

Values of α and β could be checked against measurements taken from aerial photography. In general there was good agreement between field measurements and aerial photo values for α and β (as well as with values for H taken from the avalanche atlases); however in several avalanche paths, the results were significantly different. These differences are attributed to field measurement error. Therefore the length method was used in computing the runout ratio, using data collected from aerial photography.

Assuming the data follow a Gumbel distribution (Figure 4.5 is a frequency histogram of the runout ratio data), a least squares fit to the data, on Gumbel probability paper, takes the form:

$$X_p = u + b.Y$$

where p is the non-exceedance probability, Y is the reduced variate ($Y = -\ln[-\ln[p]]$), u and b are location and scale parameters, respectively, and X_p is the runout ratio (for the chosen non-exceedance probability). Figure 4.6 presents the full data set. A simple regression was performed giving a model of the form

$$X_p = 0.021 + 0.076Y$$

with an r^2 of 0.94 and SE of 0.003.

Nixon and McClung (1993) censored their data at a reduced variate of 0. This improved the fit of the regression line and was justified since engineering applications tend to refer to the upper tail of the distribution. In this study, censoring the data in this manner provided no improvement to regression fit.

Figure 4.1 (frequency histogram of ΔX) suggests that ΔX may also follow a Gumbel distribution. A least-squares regression model fitted to the data, on Gumbel probability paper, takes the form

$$X_p = 18.3 + 36.5Y$$

with an r^2 of 0.96 and SE of 1.16. Figure 4.7 is a Gumbel plot of this data set, suggesting that ΔX approximates a Gumbel distribution. Other than providing a simpler calculation, the use of ΔX provides no benefits over using the runout ratio.

4.3.4 Outliers

In looking at frequency histograms of the data, and regression fits in the previous section, it is evident that there is an important influence from outliers on the data set. In this section, I will discuss some of the implications of these outliers and try to account for them (this section will implicitly refer to Table 4.2).

In looking at values of the runout ratio, there are several paths with runout ratios greater than 0.10 that can be considered outliers. In nearly all cases, the paths had small path length values, while retaining values of ΔX similar to other paths in the database. This made

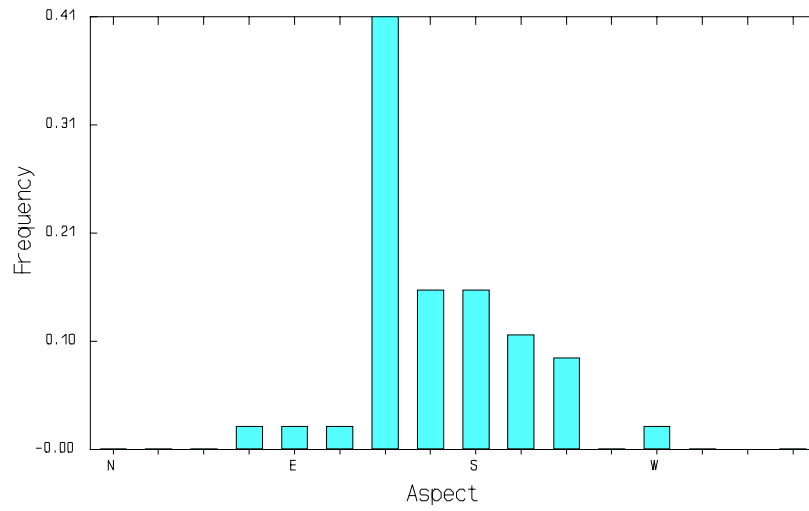


Figure 4.4 Aspect of avalanche paths, using 16 ordinal units, with N=1, S=9, E=5 and W=14 (chosen for graphical reasons). Note the high clustering of values around south.

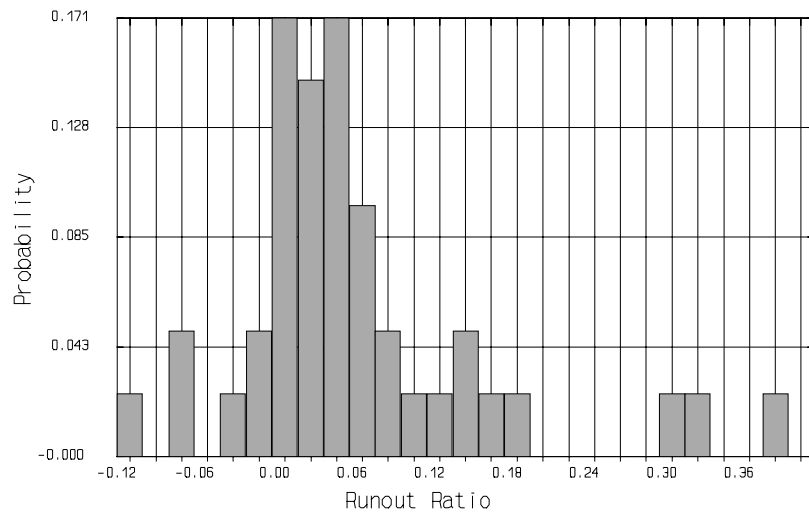


Figure 4.5 Frequency histogram of the runout ratio using the method of lengths

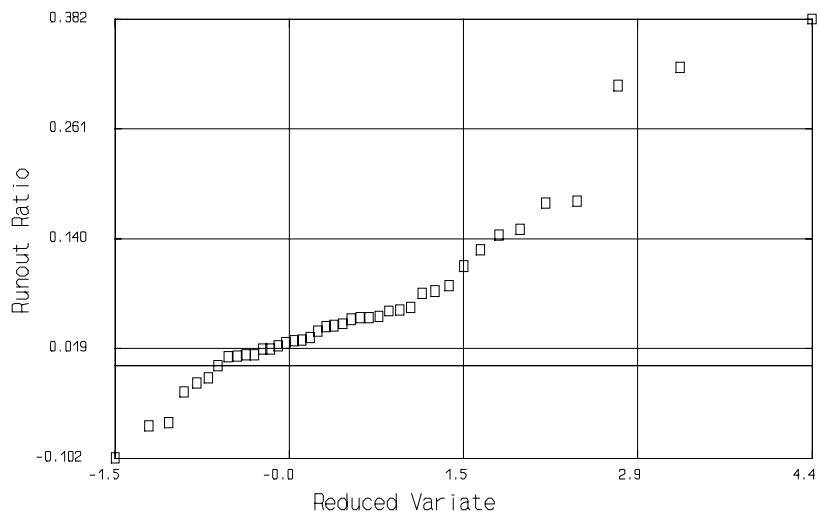


Figure 4.6 Gumbel plot of runout ratio data for the Columbia Mountains.

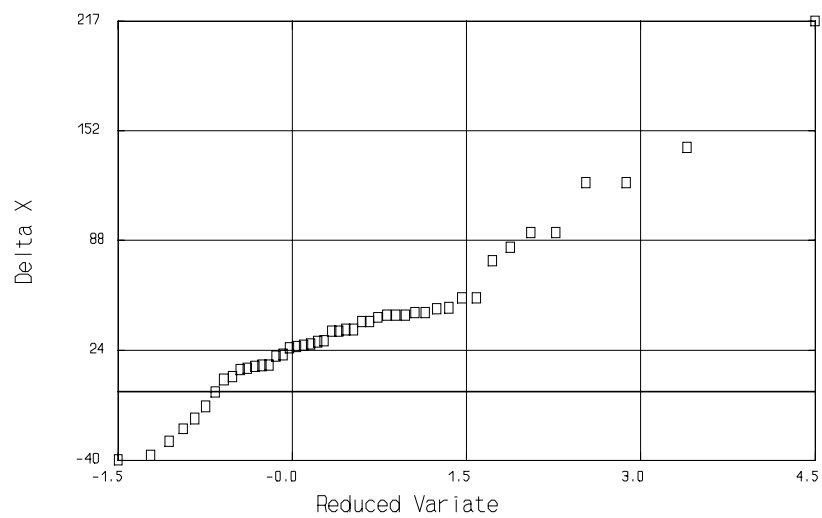


Figure 4.7 Gumbel plot of ΔX (units are in meters) data for the Columbia Mountains.

for a large runout ratio value. The three largest values, which formed a distinct group on their own, were all relatively short paths, but had large ΔX values. Interestingly these 3 paths came from Rogers' Pass; whether this is an effect of the higher elevation, and so greater snowfall, is unknown. In one case the path length was large, but had a correspondingly larger ΔX value.

In all nearly all cases with large ΔX values, the paths had large path length values (this does not imply that large paths have large ΔX values). Again, the 3 paths from Rogers' Pass formed a distinct sub-group with large ΔX values. Finally, paths with large path lengths also had large vertical drops. One path from Galena Pass also had a very high β angle, while retaining a relatively low α value. The avalanche paths at Galena Pass were noticeably short and steep, with small ΔX values.

As ΔX can be used separately as a measure of runout, it is notable that only δ ($r=0.55$) and runout zone width ($r=0.33$) were significantly correlated with ΔX . This suggests that as ΔX increases so the angle between α and β decreases and the runout zone gets wider.

4.4 CONCLUSIONS

4.4.1 Data Collection

In summary, a database of 46 high-frequency avalanche paths in the Columbia Mountains, with unobstructed runout and locatable terminus, was analyzed. Highway records of avalanche occurrence were used to determine the avalanche frequency. Due to the large proportion of monitored avalanche regions lying in the Columbia mountains, paths in these mountains alone were used in the final database. There were practical problems in locating the β -point on several paths. Following field work, aerial photography was assembled and the AP190 analytical plotter used to take further measurements.

4.4.2 Results

In this chapter, I have presented the methods of collation and collection of data for the database of high-frequency avalanche paths, both in field work and using the AP190 analytical plotter. In §4.3.1 I showed that the α angle is very steep when compared to values from low-frequency avalanche databases. More significantly, there is a small difference between α and β in this study. Consequently ΔX is small and the runout ratio is small. As a rule of thumb, the α -point will be located within $\pm 50\text{m}$ from the β -point. The mean value of δ is also large in this study, a product of the steep α angle. It is also important to note that $-\Delta X$ values were recorded on 10 of the 46 paths. Values of path length and vertical drop were also relatively small. This study has found no vertical or horizontal scale effects.

High-frequency avalanche paths in this study appear to be shorter and steeper than their lower frequency counterparts elsewhere. This basic trait has been evident in all empirical work produced on terrain characteristics. Mears (1989) summarised statistical work and showed that regions with the highest α values also had the smallest runout ratios. Avalanche dynamics work has also shown that, on a high-frequency path with a defined runout position, the basal friction coefficient (entered as $\tan\alpha$) needs to be higher. Dent (1993) has shown that increasing the depth of the avalanche, decreases the dynamic friction. As he states, *disregarding other effects, this implies that large avalanches should move faster and run out farther than small avalanches*. Steep paths may produce shallower avalanches, with increased basal friction, causing the avalanche to move slowly.

Second order polynomials and, later, orthogonal coefficients, were unable to accurately estimate ΔX . This was, in part, due to the short, steep nature of the avalanche paths. Very little curvature is present and consequently a fitted curve is unable to model the path effectively.

The regression model found track angle, catchment area, area, aspect, β , H_β and X_β

significantly correlated with α ; however when these variables were entered into a least-squares regression model, only β was significant. An alternative regression model estimating L using track angle and X_β as predictor variables provided a better fit to the data. Although useful results, 5 of the 46 paths had no locatable β -point, and therefore these cases cannot be estimated by the models. As curve fitting was unsuccessful in estimating ΔX , there were no alternative methods available to integrate data from these paths into the database. As high-frequency avalanches can be seen to stop at or around the β -point, the arbitrary choice of 10° for the location of the β -point may not be appropriate for high-frequency avalanche paths. McKittrick and Brown (1993) used an angle of 18° , however they were able to survey profiles for a small number of short avalanche paths. This method of data collection was not practical for this study. The above regression model was used to estimate the position of the 18° point, however as the profiles of the avalanche paths were so straight, estimates of ΔX were very large.

The application of the extreme-value model showed that the runout ratio approximated a Gumbel distribution. Censoring the data at the lower end (for engineering purposes) provided no better fit. It was also shown that ΔX obeyed an extreme value distribution. In order to calculate either of these parameters, it is necessary to have located the β -point. These methods are therefore unable to incorporate information from paths where β is unmeasurable.

5. STUDY OF ARRIVAL RATE

5.1 INTRODUCTION

In this chapter I present an extensive data set of 14 terrain and climate variables for 43 avalanche paths at Rogers' Pass, British Columbia, with 24 years of avalanche occurrence records for each path. All 43 paths show a high-frequency of avalanching in the range of 3 to 20 events per year.

In Chapter 1 I showed that calculations of risk increased in direct proportion to increases in event frequency. In order to properly specify the frequency component, we must know the frequency distribution of events. I show that the Poisson distribution is the most appropriate distribution. This result can then be used in calculations of risk to estimate the encounter probability for determination of the chance of encounter for a given exposure time for a given avalanche path.

Given the 14 terrain and climate (predictor) variables, I perform a multivariate correlation analysis to determine which variables are statistically significant in predicting frequency (the response variable). The analysis shows that path roughness, 30 year maximum water equivalent, location (east or west of Rogers' Pass summit), wind exposure and runout zone elevation and inclination are all significant in a multivariate sense. Inclination and elevation of the starting zone also have important single variable correlations.

The sections below contain a regional description of Rogers' Pass, a description of the data set, followed by goodness-of-fit analysis to selected probability functions. This portion of the thesis is completed with an analysis of terrain and climate factors affecting frequency.

5.2 DESCRIPTION OF ROGERS PASS AND DATA

The data set used for this analysis comes from Rogers' Pass, British Columbia, Canada. The area is located within Glacier National Park. The Canadian Parks Service maintains avalanche control on most of the 134 avalanche paths over a linear highway distance of 45km. Heavy snowfall and steep terrain are combined, making it an area of high avalanche frequency. The eastern side of the pass is relatively U-shaped with up to 1650m of relief. The western side is more V-shaped with relief up to 1800m.

The Selkirk Ranges occupy the interior wet belt of British Columbia receiving the second greatest recorded level of precipitation in Canada. Warm westerly storm tracks produce a deep snowpack that is able to cling to steep slopes, establishing a potential for large destructive avalanches. There are, however, periods of cold, stable air which can dominate Rogers' Pass for long periods. Schliess (1989) recognised three climatological sub-zones: the west side, the summit and the east side. The west side is distinguished by heavy snowfall and mild temperatures, while the east side has lighter snowfall and colder temperatures. The summit area produces a mixture of unstable weather.

Not until after the completion of the Trans-Canada Highway were detailed records of avalanche occurrence maintained. During the winter of 1967 the National Research Council (NRC) began recording avalanche occurrence. Some paths ceased to be monitored after 1984, with most ending in 1989. The aim in monitoring avalanches was to record all "major" occurrences, particularly those that ran into the valley. In the late 1970's the Canadian size-classification scheme (McClung and Schaerer, 1981) was incorporated into the observations. In general, only avalanches greater than size 2 were recorded. The data set can be considered accurate and provides the best description of avalanche activity so far analysed.

The Rogers' Pass data used in this thesis were split into two sections. The first set contains 14 paths with continuous good quality data records from 1967 to 1989. The second set contains 29 paths, however, the data are incomplete (there are missing values); in this case the missing values were ignored before the analysis was performed on the remaining data. In general, for the period 1967-1989, less than 20% of data were missing when all paths are taken into account.

5.3 FREQUENCY ANALYSIS - GOODNESS OF FIT

In order to determine how the frequency data relate to a probability mass function or probability density function it is appropriate to apply statistics for goodness-of-fit. For this study the chi-square test, using classes with a minimum expected frequency of 2 (Roscoe and Bryars, 1971; see also d'Agostino and Stephens, 1986 for a further discussion), and testing at the 0.05 significance level, was used.

The frequency of avalanches may be thought of as a series of discrete, rare, independent events. This matches the conditions for a Poisson experiment and so is the appropriate distribution to test the frequency data with for goodness-of-fit. These conditions may be violated for high event frequency avalanche paths as the probability of avalanching will be related to the occurrence of earlier avalanches. An example of the violation of the assumption of independent events would be the recharge rate of snow in the starting zone in one winter season. A normal distribution can approximate the Poisson distribution when the Poisson parameter (μ) is greater than 9; therefore testing for goodness-of-fit using a normal distribution is appropriate. As μ becomes larger the discrete nature of the data becomes less important. This assumes that both upper and lower values, 3 standard deviations from the mean, are positive (as it is not possible to have negative event frequencies).

Figure 5.1A shows a Poisson distribution fitted to one path from Rogers' Pass. This path shows a satisfactory fit, however Figure 5.1B is an example of a path where the Poisson fit failed the chi-square test.

Results of the chi-square tests, for both the complete and incomplete data sets, show that both the Poisson and normal distributions provide a satisfactory fit to most of the data for the 43 avalanche paths. However, in several cases both the Poisson and normal fail the test. Table 5.1 provides a frequency table of chi-square test results. It is notable the normal distribution provides a better fit than the Poisson distribution at $\mu > 14$, although at lower values of μ both perform equally well. A visual inspection of the goodness-of-fit of the Poisson distribution to the avalanche data showed that the Poisson provided a better fit at lower values of μ .

This picture is further complicated by the use of artillery which artificially increases the frequency of avalanche events. Of the 43 paths, 7 have received artillery control since the highway was completed, with a further 5 having received control more recently. Of the former 7, 5 have mean frequencies greater than 9 avalanches per year, with 4 of these greater than 14. As only 10 paths have means greater than 14 avalanches per year, this is an important effect upon overall path frequency. Not all the paths follow this general trend, however. As depicted earlier, Figure 5.1B is an example of a poor fit to a Poisson distribution. The plot shows a lack of data points in the central area of the distribution, while there are several notable outliers.

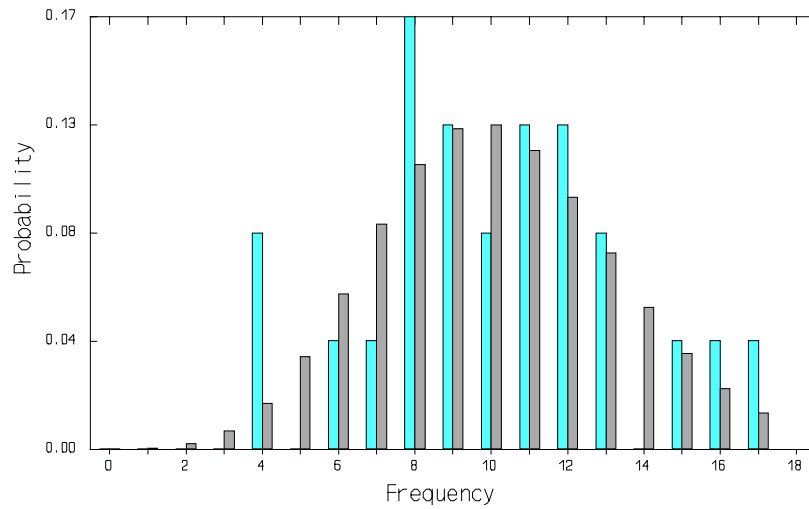


Figure 5.1A Avalanche frequency for Cougar Corner 2 (light) fitted to a Poisson distribution (dark). This path has a frequency of 10.1 events per year. Results of Chi-square test were: Degrees of Freedom 7, Chi-Square Statistic 2.55 and Significance Level **0.923**

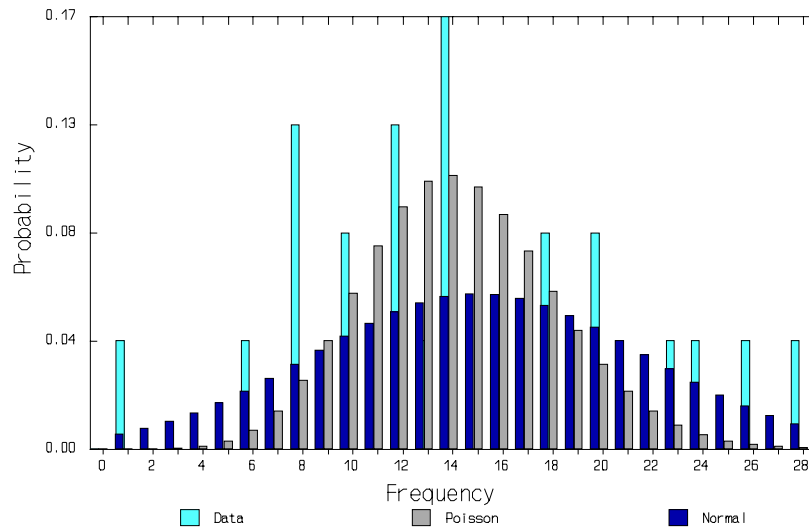


Figure 5.1B Avalanche frequency for Tupper Cliffs fitted to a Poisson and normal distribution. This path has a frequency of 6.2 events per year. Results of Chi-square test:

	Normal	Poisson
Degrees of Freedom	7	7
Chi-Square Statistic	8.30	18.5
Significance Level	0.307	0.010

		Avalanche Frequency			
		0-5	5-9	9-14	>14
Poisson	Pass	4	14	10	7
	Fail	0	3	2	3
Normal	Pass	4	14	11	10
	Fail	0	3	1	0
# of points		4	17	12	10

Table 5.1 Frequency table of chi-square test passes and fails (at 0.05 significance) using the equal-interval method, by avalanche path frequency, for normal, Poisson and chi-square distributions.

Terrain Variables	Mean	Standard Deviation	Range
path slope (°)	33.8	2.6	12
track slope (°)	38.5	3.6	15
start zone slope (°)	38.2	5.0	25
runout zone slope (°)	21.2	5.7	30
vertical drop (m)	922	251	965
path length (m)	1676	443	1965
starting zone elevation (m)	2041	248	990
runout zone elevation (m)	1114	109	440
*aspect (1-16)	6.0	4.2	12
area of catchment (ha)	18.5	15.8	65.6
*wind exposure	3.1	1.0	4
location (km)	-0.8	5.9	20.7
30 year maximum water equivalent (m)	1.4	0.3	1.2
*roughness	0.25	0.06	0.30

Table 5.2 Predictor variables and descriptive statistics of data used in the regression analysis. See text for definition of categorical variables denoted by (*).

Although the frequency for this path is 14.3 events per year, the effect of some years having no avalanches and some years with 28 avalanches causes a fitted Poisson curve to fail the test. The Poisson underestimates at the peak and in the tails. The normal, although underestimating the peak, provides a better estimate in the tails. These differences partially cancel out in the chi-square test itself, enabling the normal curve to fit data.

In summation, I have shown that the Poisson and normal distributions are both able to fit the data. However the Poisson distribution gives a satisfactory fit to most of the avalanche data and it is the most appropriate distribution since the frequency of avalanches may be thought of as a series of discrete, rare, independent events, which matches the conditions for a Poisson experiment. However, at the higher values of μ (>14) the normal is better able to model the variability that is currently displayed in the avalanches I have analysed. This variability may be attributed to the use of artillery, in combination with effects of outliers. A greater sample size would allow a more definite answer to this question.

If the Poisson distribution is chosen as the most appropriate distribution, it is possible to use μ (mean of each data set) for each of these paths as characteristic of the path frequency. Variations in μ may be attributed to changes in terrain parameters and climate; however the extent of influence that each of these factors introduces is unknown. The following section presents an analysis of terrain features for the paths from Rogers Pass.

5.4 RELATION BETWEEN FREQUENCY AND TERRAIN PARAMETERS

Previous work carried out on data from Rogers' Pass has provided a variety of terrain parameters that have been used in this work. Schaerer (1977) analysed avalanche frequency (using 9 years of data) on 36 of the 43 avalanche paths analysed here, collecting data on 16

terrain and climate variables. He then attempted to correlate the avalanche frequencies with the terrain parameters.

A limiting factor in Schaerer's (1977) work was the small data record: only 9 years of avalanche events. Given the small size of the data set used to calculate the mean frequencies, the effect of outliers on the results could well be significant. In the present study, I was able to use 24 years of records on the 43 paths originally contained in the National Research Council data set. These produced a mean frequency of 10 avalanches per year with a standard deviation of 4.5 per year. The minimum was 3 avalanches per year and the maximum 21 avalanches per year.

Schaerer (1977) noted that there is a variation in climate depending on location at Rogers' Pass. Snowfall on the east side of the pass is about 80% of that at an equal elevation on the west side. However, he suggested that paths on the east side have higher starting zones and so may receive snowfall comparable to those on the west side. The present work has introduced a location parameter and several elevation parameters to take into account these climatic effects. Figure 5.2 shows the location of paths east-west of Rogers' Pass summit with respect to avalanche frequency.

Table 5.2 shows the terrain parameters, and descriptive statistics, used in the following regression analysis. Several variables require further explanation:

(1) 30 year maximum water equivalent - this variable is based on snow depth measurements taken near Rogers' Pass. Figure 5.3 shows the 30 year maximum water equivalent plotted against avalanche frequency. Over a period of between 15 and 20 years, maximum snow depth measurements were taken once a year at 6 stations increasing in elevation on both the east and west side of the pass. This was then converted to water equivalent. The snow depth measurements were graphed against elevation, giving a clear relationship. The 30 year

maximum water equivalent was calculated from the cube-root normal distribution for the centre of each of the avalanche path catchments to give an estimate appropriate for a given catchment elevation.

(2) Wind Index - a qualitative index of the magnitude of snow drifting that can be expected in the avalanche starting zone (Schaerer, 1977):

- 1 Starting zone completely sheltered from wind by surrounding dense forest.
- 2 Starting zone sheltered by an open forest or facing the direction of the prevailing wind.
- 3 Starting zone an open slope with rolls and other irregularities where local drifts can form.
- 4 Starting zone on the lee side of a sharp ridge.
- 5 Starting zone on the lee side of a wide, rounded ridge or open area where large amounts of snow can be moved by wind.

Figure 5.4 shows wind index plotted against avalanche frequency.

(3) Roughness - expressed as the water equivalent of snow required to cover rocks, shrubs and ledges in starting zones before avalanches will run. Figure 5.5 shows roughness plotted against avalanche frequency.

(4) Aspect - measured in 16 ordinal units. Figure 5.6 shows a plot of aspect with avalanche frequency; due to the clustering of northerly and southerly aspects, the data were ranked as either 1 (north) or 2 (south).

(5) Location - straight line distance in kilometres, east-west from the Rogers' Pass summit to where the path dissects the highway (see Figure 5.2).

In reviewing the descriptive statistics for the avalanche paths in Rogers' Pass, some values can be compared with avalanche path regions in Appendix 3. The avalanche paths are very steep, with a mean path slope of 33.8° (this can be compared directly to the α -angle for avalanche regions in Appendix 3). There is also a high mean vertical drop (950m). Runout

zone elevation, in comparison to starting zone elevation, has a low range and SD, a result of the relatively small increase in elevation of the highway as it traverses the pass. As previously noted, starting zone elevations are different on the east and west side of the pass, accounting for the variation in starting zone elevation. The aspect of avalanche paths at Rogers' Pass is predominantly northerly or southerly, a result of the east-west alignment of the pass.

Initially a Pearson product moment correlation matrix was compiled for the 14 variables against avalanche frequency (F). Results indicated that the following variables were significantly correlated with avalanche frequency:

	r-value
runout-zone elevation (RE)	0.47
roughness (R)	-0.57
30 year maximum water equivalent (MWE)	0.54
wind index (W)	0.45
location (L)	0.48
runout-zone slope (RS)	0.33

Other variables which showed high correlations, but were not significant, were starting zone slope and elevation. A multiple stepwise regression was then performed on the above 8 variables, giving a model of the form:

$$F = 14.02 - 33.03R + 1.39W + 0.03L$$

with an r^2 of 0.57 and a standard error (SE) of 2.93.

In order to remove anthropogenic affects on avalanche frequency, all avalanche paths that had received explosive control were removed from the data set. A Pearson product moment correlation matrix, compiled for the 14 variables against avalanche frequency,

indicated that the following variables were significantly correlated with avalanche frequency:

	r-values
runout zone slope (RS)	0.39
runout zone elevation (RE)	0.47
aspect (A)	0.52
roughness (R)	-0.65
30 years maximum water equivalent (MWE)	0.70
wind index (W)	0.49
location (L)	0.44

A stepwise regression, on the remaining 26 avalanche paths, gave a best regression of the form:

$$F = -5.22 + 0.01RE - 26.9R + 5.0MWE$$

with an r^2 of 0.66 and a SE of 2.70. In this equation, the variance of the residuals was not constant (see Figure 5.7) and so a log transformation was performed on the avalanche frequency. This transformation reduced the standard error and slightly increased the r^2 (see Figure 5.8). This gave a best regression of the form:

$$\log(F) = 0.36 + 0.001RE - 2.75R + 0.66MWE$$

with an r^2 of 0.75 and a SE of 0.25.

Both the full data set and the data set censored with respect to explosive control, were partitioned with respect to avalanche path location east or west of the Rogers' Pass summit. Generally, variables significantly correlated with avalanche frequency were R, MWE and W for both the east and west sides. However, the censored data set for the west side had a strong correlation with MWE ($r=0.82$), perhaps due to the low change in elevation of the catchment area for avalanche paths in this region. Interestingly, the full data set for the west

side had a correlation, not found in the other partitioned data sets, with starting zone slope.

Inspection of the regression equations indicates the importance of climate to avalanche frequency. The supply of snow is entered into this study as W and MWE . Both RE and L are related to snow supply. Runout zone slope, aspect and roughness appear to be the only terrain variables affecting avalanche frequency.

5.5 DISCUSSION AND CONCLUSIONS

In this chapter I have analyzed avalanche frequency and attempted to account for their variations with respect to terrain and climate. The chi-square test performed satisfactorily; however there was difficulty in distinguishing between a normal and a Poisson distribution due to similarity between these distributions when $\mu > 9$. Given that avalanche frequency is a series of rare, discrete, independent events the Poisson distribution seems to be the most appropriate distribution. When $\mu > 14$, a normal distribution may be preferred by some since it has two parameters and, therefore, more flexibility to fit the data.

This result has several important implications for future research. In risk mapping it is now possible to use the Poisson distribution in the calculation of the encounter probability (see §3.1). This result can then be used in as P_h for the calculation of specific risk (P_s) for a given location. This analysis is therefore able to recommend the use of the Poisson distribution in future land-management studies.

In the second half of this chapter I concentrated on an analysis of terrain and climate with respect to avalanche frequency. Schaerer (1977) found roughness, wind exposure, fracture point incline (not used in this study) and incline of track to be significantly correlated with frequency, suggesting that climate variables (roughness and wind exposure), along with

terrain parameters (fracture point incline and track incline) are the most important variables affecting frequency. Climatic conditions in the starting zone are important here, as are fracture point and track inclines.

This study presented roughness, maximum water equivalent and location in the final regression model for the full data set. Censoring the data, with respect to explosive control, presented runout zone elevation, roughness and maximum water equivalent in the final regression model. As maximum water equivalent and location are related to snow fall supply, avalanche frequency appears to be strongly related to climate; however both roughness and runout zone elevation are significant terrain variables. Runout zone slope and aspect also have important effects upon avalanche frequency.

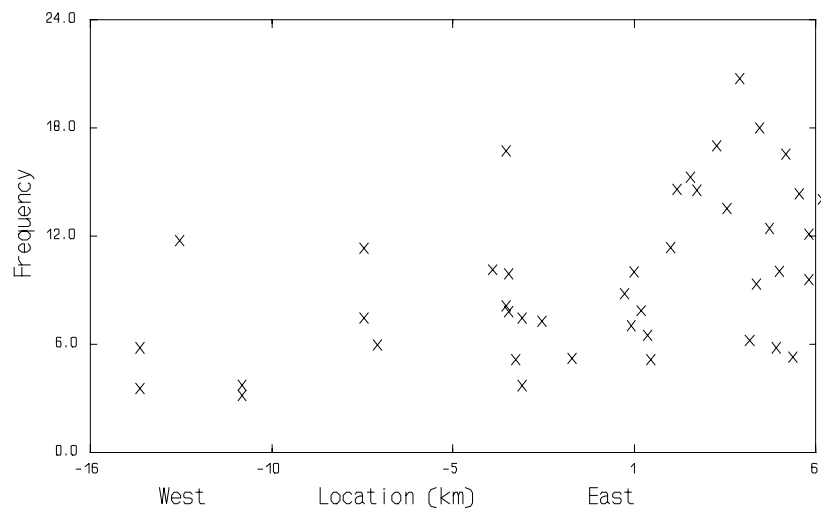


Figure 5.2 Location of avalanche paths at Rogers Pass with respect to avalanche frequency. Location is calculated as distance (km) east-west of the Rogers Pass summit (designated as 0) where the centre of the path dissects the Trans-Canada Highway. Negative location is east of Rogers' Pass and positive is west.

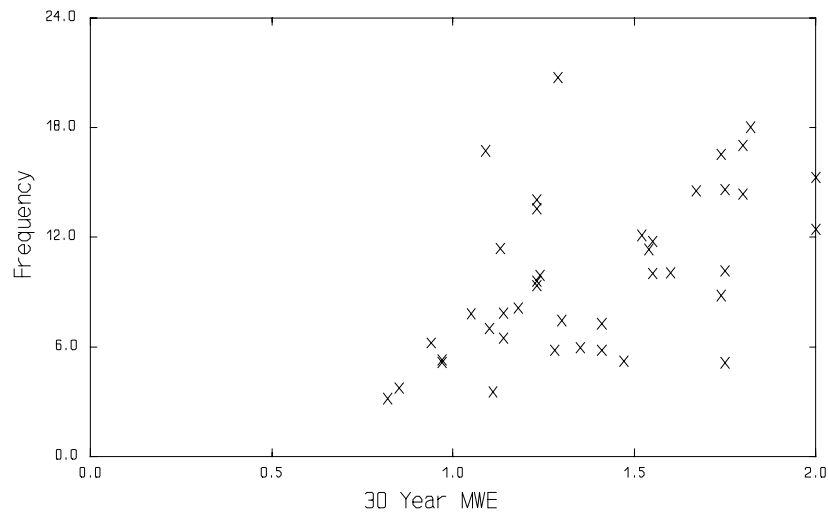


Figure 5.3 30 year maximum water equivalent plotted against avalanche frequency. Maximum snow depth measurements at 6 different elevations on the east and west side of Rogers Pass are highly correlated with elevation. This relationship is used to calculate the maximum water equivalent for the centre of the catchment for each path and then, using a cube root normal distribution, the 30 year maximum is calculated.

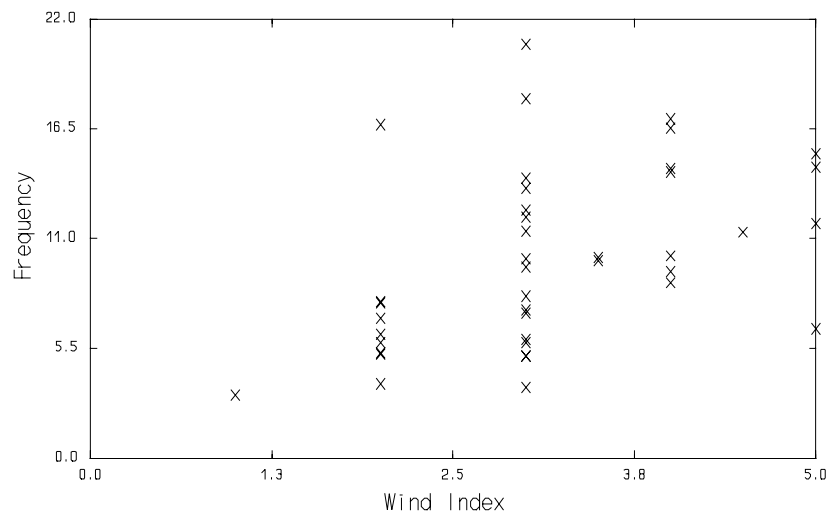


Figure 5.4 Wind Index plotted against avalanche frequency, where the Wind Index is a qualitative index of the magnitude of snowdrifting that can be expected in the avalanche starting zone.

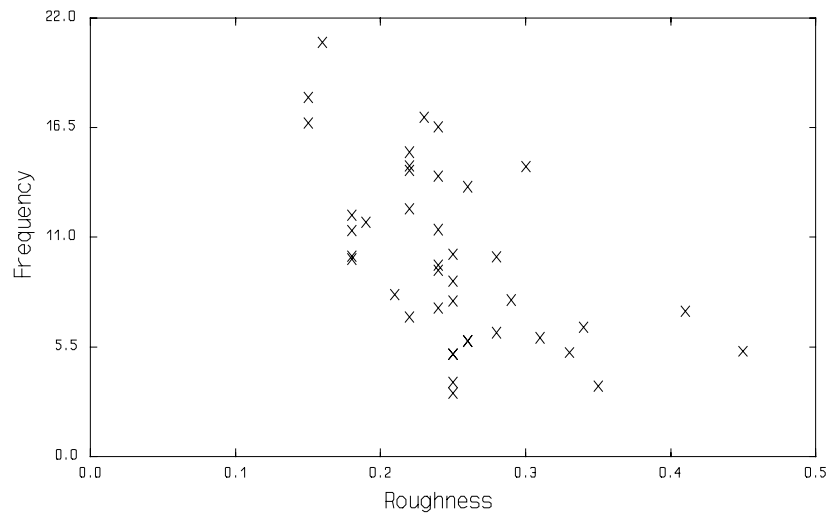


Figure 5.5 Roughness as a function of avalanche frequency, where roughness is the water equivalent of snow required to cover rocks, shrubs and ledges before avalanches will run. A negative correlation is displayed here: as the roughness in the starting zone increases, so the frequency decreases.

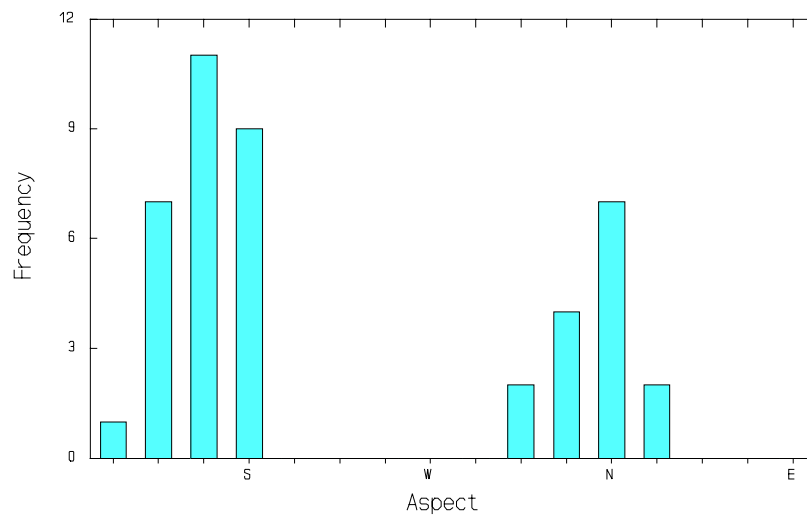


Figure 5.6 Aspect of avalanche paths, using 16 ordinal units. Note the high clustering of values around south and north. For the regression analysis, each path was assigned a categorical value of either northerly or southerly.

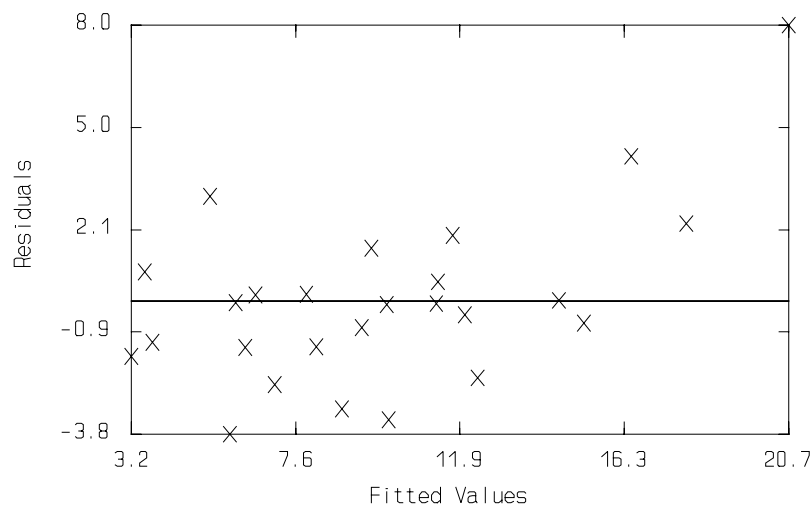


Figure 5.7 Plot of the residuals versus the predicted values for the stepwise multiple regression, using avalanche frequency as the dependent variable. The pattern indicates that the variance of the multiple regression residuals is not constant.

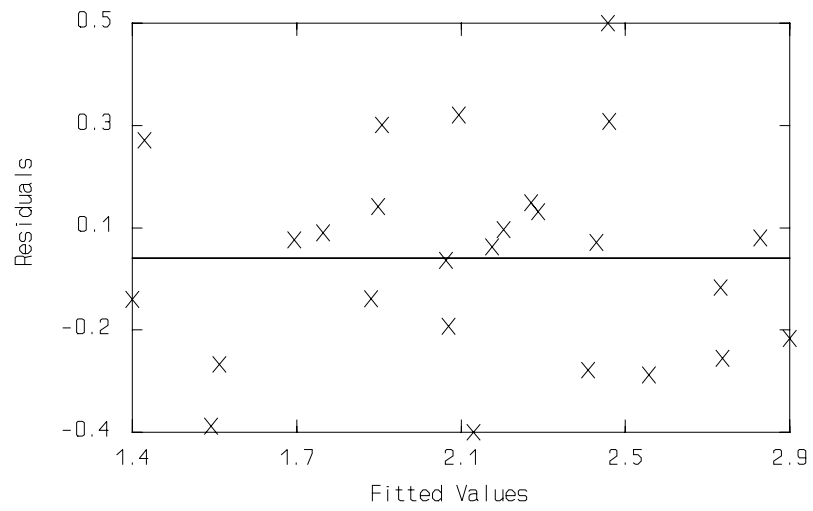


Figure 5.8 Plot of the residuals versus the predicted values for the stepwise multiple regression, using a log transformation of the avalanche frequency as the dependent variable.

6. CONCLUSIONS

6.1 INTRODUCTION

This thesis is a study of high-frequency avalanche paths with respect to predicting extreme runout and the effect of terrain and climate on avalanche frequency. I have presented a review of work on avalanche extreme runout and the use of different probability distributions to describe avalanche magnitude and frequency. The second portion of this thesis presents results from current research into high-frequency avalanching. This work was split into two sections that, although separate, have important consequences for land use management in terrain threatened by avalanches. The first section was concerned with modelling the extreme runout of high-frequency avalanches paths, while the second section dealt with testing the applicability of different probability distributions for use in avalanche risk calculations and a study of the relationship between avalanche frequency and different likely predictor variables.

In this final review chapter I will briefly summarise important elements from review chapters, placing these points within the framework of results from Chapters 4 and 5. Although Chapters 4 and 5 already have concluding sections, it is important to reiterate these findings and place them in context.

6.2 THESIS REVIEW

In the first chapter I introduced the problem of avalanche terrain and the hazardous nature of human interactions with this environment. These interactions may be for reasons of transportation, recreation or habitation. Common to all is the inherent risk associated with operating in such an area. Risk was defined probabilistically, with an emphasis on the high risk associated with higher frequency avalanches. Given this higher risk, an understanding

of the probabilistic nature of high-frequency avalanches is important, as is the nature of terrain associated with these avalanches, particularly with respect to runout. Although much work has previously been produced on avalanches and avalanche terrain, most previous studies were either descriptive or focused on low-frequency avalanches.

In chapter 2 I gave a detailed review of the prediction of extreme (low-frequency) avalanche runout. An initial section focused on physical modelling, however, due to the problems associated with defining boundary conditions, this is an unsuitable tool for runout prediction. More recently, statistical modelling has emerged as a more practical solution for land management problems. Two main approaches have been utilised in zoning land with respect to runout. Lied and Bakkehøi (1980) produced the first definitive study of avalanche runout, using different terrain parameters in multiple regression models to define runout. This, and subsequent work, showed that the β angle was highly correlated with runout (defined as the α angle). Although other variables were significantly correlated with α , when entered into a regression model, little more explanation, in terms of variability, was added. Subsequent work by McClung and Lied (1987), introduced the runout ratio which was shown to follow a Gumbel distribution. McClung and Mears (1991) went onto model data from 5 different mountain ranges, demonstrating that differences between maritime and continental regional climates were not the cause for differences between runout for these mountain ranges. The extreme-value model has been used in conjunction with physical models to provide an effective method of avalanche zoning.

A review of work on avalanche magnitude and frequency, and the effect of interactions between climate and terrain on avalanche frequency, was given in Chapter 3. If information on avalanche frequency, particularly for high-frequency avalanches, is to be used in risk mapping then the probability of occurrence must be calculated from a probability density function or probability mass function. Good, long term, records of avalanche

occurrence are needed in order for this to be formulated. This is the biggest problem facing the avalanche researcher and is demonstrated by the difficulties faced by Fitzharris (1977) and Föhn (1975) in their work. Both studies dealt with low-frequency avalanche paths and faced problems of data quality. The chapter then went on to describe the importance of separating the effects of climate and terrain, on avalanche frequency.

Chapter 4 presented a database of 46 high-frequency avalanche paths from the Columbia Mountains in British Columbia, with information on runout and other terrain parameters. These data were acquired from field measurements and air photo interpretation. Descriptive statistics showed that these paths are steeper, on average, than low-frequency paths. Also important was the proximity of the α -point to the β -point, implying short runout. The runout ratio was also noticeably low, due to the small differences between α and β .

In nearly a quarter of cases the avalanche path ended before a local slope angle of 10° was reached. This meant missing values in the database as some of these paths had unmeasurable terrain parameters, whilst there was a lack of confidence in others. In order to resolve this, a second order polynomial, using orthogonal polynomial coefficients, was used to model the centre line profile of each of these paths and therefore estimate the position of the β -point. Unfortunately these estimates were unsatisfactory and so this problem was not resolved; a possible solution is to use a different slope angle to define β . This method has been successfully used by McKittrick and Brown (1993) for their database of low-frequency avalanche paths in south-west Montana.

A regression model, using the above terrain parameters, found β to be the most highly correlated variable with α ($r^2=0.59$). An alternative regression model, estimating horizontal path length (L), was highly found to be highly correlated with track angle and X_β , providing a better fit to the data than the single parameter model used to estimate α . The use of these

models is limited given that several paths have no β value recorded for them. Following this, the runout ratio was shown to follow a Gumbel distribution. Censoring the data provided no better fit to the data. The parameter ΔX was also shown to follow a Gumbel distribution. Nixon and McClung (1993) suggest that the extreme-value model provides better estimates of ΔX than the regression model. They found that the extreme-value model, at $P=99\%$, provided larger estimates of ΔX when compared to the regression model, while at $P=50\%$ estimates of ΔX were smaller.

In Chapter 5 I introduced work on the fitting of different probability distributions to 24 years of avalanche occurrence data from Rogers' Pass, British Columbia. The avalanche occurrence records were available for 43 separate avalanche paths. This represents this most comprehensive survey of high-frequency avalanche paths so far completed. I recommend the use of the Poisson distribution at low values of μ (<9). At higher values of μ , the effect of discrete data becomes less important with better results being achieved by the normal distribution.

This result has important implications for risk mapping, as it is now possible to stipulate the Poisson distribution in the calculation of the encounter probability to define P_h in the calculation of specific risk (P_s) for a given location. Even with 24 years of records on high-frequency paths, several paths showed unsatisfactory fits due to a lack of data.

Chapter 5 also contains an examination of variations in frequency of avalanche paths in terms of terrain and climate variables. As Rogers' Pass is contained within one regional climate, variations in frequency should be due to changes in terrain. A Pearson product moment correlation matrix showed that runout zone elevation, roughness, 30 year maximum water equivalent, wind exposure, location and runout zone inclination were significantly correlated with avalanche frequency. These variables were then entered into a multiple

stepwise regression which produced the three parameter model with roughness, wind index and location.

The data were then censored with respect to explosive control and significantly correlated predictor variables were entered into a regression model. This presented runout zone elevation, roughness and maximum water equivalent in the final regression model. However, as the variance of the residuals was not constant, a log transformation was applied to avalanche frequency and a further regression performed. This had the effect of increasing the r^2 and reducing the SE for the same predictor variables.

Avalanche frequency appears to be strongly related to climate, as maximum water equivalent, wind index and location are all related to snow fall supply. However roughness, runout zone elevation, runout zone slope and aspect all have important effects upon avalanche frequency.

6.3 FINAL REVIEW AND RECOMMENDATIONS

In this thesis I have presented a review and results from current research into the nature of high-frequency avalanches. Previous research has concentrated mostly on low-frequency avalanches; however high-frequency avalanches are very important for risk management in avalanche terrain.

Although the two research chapters in this thesis are separate entities, they represent two important aspects of high-frequency avalanche paths. For risk mapping purposes, it is frequency that controls risk, in a probabilistic sense. On high-frequency paths it is now possible to stipulate a probability density function or probability mass function and so calculate the encounter probability as input to the calculation of specific risk. I have also attempted to explain frequency at Rogers' Pass in terms of changes in path terrain variables and climate parameters; however micro-climate was the dominant factor.

I have also shown that high-frequency avalanches are typically found on steep slopes, as the mean value of α was 33.3° . As the α -point and β -point are often found in close proximity, there is a tendency for the extreme runout limit to be located near the 10° slope angle. As a simple management rule, the location of extreme runout for high-frequency avalanches can be found within $\pm 50\text{m}$ of the β -point. These results verify similar conclusions reached from work on low-frequency avalanches as well as with physical models. The higher mean value of α for the data in this study, when compared to low-frequency avalanche data, suggests higher basal friction coefficients for snow. Dent (1993) suggests that shallow flow depths increase the friction coefficient and so leads to a shorter extreme runout. However, these are tentative conclusions; further research could use records of avalanche occurrence to analyse avalanche magnitude, frequency and runout for the paths in this study. This may highlight important elements involved in the generation of high-frequency avalanches. Entrainment and the snow retention capacity of the path may have important effects, but they have not been quantified based on field measurements.

Just as regional climate is likely to be an important effect on avalanche frequency between avalanche regions, micro-climate has been shown to be more dominant within the avalanche region at Rogers' Pass. Further research should be concentrated on using terrain variables (such as catchment capacity) and climate variables to account for changes in frequency, as much of the frequency variance remains unexplained.

NOMENCLATURE

Absolute orientation - process of entering UTM coordinates into the stereo model created during *relative orientation*.

Design-avalanche magnitude - magnitude of avalanche mitigated against in a hazardous region. The proposed land use, personnel exposure, cost of facility and risk tolerance all have to be considered.

Encounter probability - probability of at least one avalanche occurring within a designated return period.

Hazard line - the boundary of large infrequent avalanches (Freer and Schaerer, 1980).

Hazard zone analysis - procedure to delimit an area into zones of decreasing risk.

Magnitude probability - probability of at least one magnitude avalanche occurring within a designated return period.

Relative orientation - process of mathematically, optically or mechanically removing the effects of relief and radial displacement from aerial photography.

Return period - reciprocal of the annual probability (frequency) of an avalanche occurring within a set time period.

Runout ratio - a dimensionless scaling parameter, $\Delta X/X_B$ (see Figure 2.2).

Runout zone - area on an avalanche path of deceleration and deposition of material.

Starting zone - area on an avalanche path of snow accumulation, usually allowing the initiation and acceleration of avalanches.

Track - area on an avalanche path of maximum velocity.

Yield Ratio - the proportion of yielded avalanche snow to total snowfall for an avalanche path.

BIBLIOGRAPHY

Allix, A. (1924) "Avalanches." *Geographical Review* V14, p519-560

Bakkehoi, S., Cheng, T., Domaas, U., Lied, K., Perla, R. and Schieldrop, B. (1981) "On the computation of parameters that model snow avalanche motion." *Canadian Geotechnical Journal*, V18, p121-130

Bakkehoi, S., Domaas, U., and Lied, K. (1983) "Calculation of snow avalanche runout distance." *Annals of Glaciology*, V4, p24-29

Bakkehoi, S. (1987) "Snow avalanche prediction using a probabilistic method." *Proceedings of Davos Symposium*, p549-555

Björnsson, H. (1980) "Avalanche activity in Iceland, climatic conditions and terrain features." *Journal of Glaciology*, V26, p13-23

Bovis, M.J. and Mears, A.I. (1976) "Statistical prediction of snow avalanche runout from terrain variables." *Arctic and Alpine Research*, V8, p115-120

Burkard, A. and Salm, B. (1992) "Die bestimmung der mittleren anrissmächtigkeit d_0 zur berechnung von fließlawinen." *Eidg. Institut für Schnee- und Lawinenforschung* Nr. 668

Burrows, C. and Burrows, V. (1976) "Procedures for the study of snow avalanche chronology using growth layers of woody plants." *University of Colorado, Institute of Arctic and Alpine Research, Occasional Paper 23*

Buser, O. and Frutiger, H. (1980) "Observed maximum runout distance of snow avalanches and the determination of the friction coefficients μ and ξ ." *Journal of Glaciology*, V26, p121-130

Butler, D.R. and Malanson, G.P. (1985) "A history of high-magnitude snow avalanches, South Glacier National Park, Montana, USA." *Mountain Research and Development* V5, p175-182

Butler, D.R. and Walsh, S.J. (1990) "Lithologic, structural and topographic influences on snow-avalanche path location, Eastern Glacier National Park, Montana." *Annals of the Association of American Geographers*, V80, p362-378

Carrara, P.E. (1979) "The determination of snow avalanche frequency through tree ring analysis and historical records at Ophir, Colorado." *Geol. Soc. of America Bulletin*, V90, p773-780

Cartwright, J., Boyne, H. and Williams, K. (1990) "Computer assisted identification of potential avalanche terrain." *Proceedings of the International Snow Science Workshop, Bigfork, Montana (Abstract)*, p38

Colbeck, S.C. (1980) Dynamics of snow and ice masses. *Academic Press, London*

- D'Agostino, R. and Stephens, M.** (1987) Goodness of Fits Techniques *Dekker, New York*
- Dent, J.R** (1993) "The dynamic friction characteristics of a rapidly sheared granular material applied to the motion of snow avalanches." *Annals of Glaciology*, V18, p215-220
- Epp, M. and Lee, S.** (1987) Avalanche Awareness *Wild Side, London*
- Ferguson, S.A., Moore, M.B., Marriott, R.T. and Kramer, K.** (1990) "Northwest avalanches." *Proceedings of the International Snow Science Workshop, Bigfork, Montana (Abstract)*, p302
- Fitzharris, B.B. and Schaerer, P.A.** (1980) "Frequency of major avalanche winters." *Journal of Glaciology*, V26, p43-52
- Fitzharris, B.B.** (1981) "Frequency and climatology of major avalanche winters at Rogers Pass, 1909 to 1977." *National Research Council Canada, DBR Paper No.956*
- Föhn, P.** (1975) "Statistische aspekte bei lawineneignissen." *Internationales Symposium Interpraevent 1975, Innsbruck, Band 1; Sonderdruck*, p293-304
- Föhn, P.** (1979) "Avalanche frequency and risk estimation in forest sites." In *"Mountain forest and avalanches, International Union of Forestry Research Organizations, Proceedings of Davos Seminar*
- Föhn, P. and Meister, R.** (1981) "Determination of avalanche magnitude and frequency by direct observations and/or with the aid of indirect snowcover data." *IUFRO/FAO Colloquium on Research on Small Torrential Watersheds, Grenoble*
- Fraser, C.** (1966) Avalanche Enigma *Murray*
- Freer, G.L. and Schaerer, P.A.** (1980) "Snow-avalanche zoning in British Columbia." *Journal of Glaciology*, V26, p345-354
- Frutiger, H.** (1990) "Maximum avalanche runout mapping; a case study from the central Sierra Nevada." *Proceedings of the International Snow Science Workshop, Bigfork, Montana*, p245-250
- Fujisawa, K., Tsunaki, R. and Kamiishi, I.** (1993) "Method of estimating snow avalanche runout distance with topographic data." *Annals of Glaciology*, V18, p239-244
- Gray, D.M. and Male, D.H.** (1981) Handbook of Snow *Pergamon, Toronto*
- Hungr, O. and McClung, D.M.** (1987) "An equation for calculating snow avalanche runup against barriers." *Proceedings of Davos Symposium IAHS Publ. No. 162*, p605-612
- Lied, K. and Bakkehoi, S.** (1980) "Empirical calculations of snow-avalanche run-out distance based on topographic parameters." *Journal of Glaciology*, V26, p165-178

- Lied, K. and Toppe, R.** (1989) "Calculation of maximum snow avalanche runout distance based on topographic parameters identified by digital terrain models." *Annals of Glaciology*, V13, p164-169
- McClung, D.M. and Schaerer, P.** (1981) "Snow avalanche size classification." *Canadian Avalanche Committee, Ed. Proceedings of Avalanche Workshop, Nov. 3-5, 1980. Associate Committee on Geotechnical Research, Technical Memorandum 133. Ottawa: National Research Council of Canada*, p12-27
- McClung, D.M. and Schaerer, P.A.** (1983) "Determination of avalanche dynamics friction coefficients from measured speeds." *Annals of Glaciology*, V4, p170-173
- McClung, D.M. and Schaerer, P.A.** (1985) "Characteristics of flowing snow and avalanche impact pressures." *Annals of Glaciology*, V6, p9-14
- McClung, D.M.** (1987) "Mechanics of snow slab failure from a geotechnical perspective." *Proceedings of Davos Symposium IAHS Publ. No. 162*, p475-507
- McClung, D.M. and Lied, K.** (1987) "Statistical and geometrical definition of snow avalanche runout." *Cold Regions Science and Technology*, V13, p107-119
- McClung, D.M., Mears, A.I. and Schaerer, P.A.** (1989) "Extreme avalanche run-out: Data from four mountain ranges." *Annals of Glaciology*, V13, p180-184
- McClung, D.M.** (1990) "A model for scaling avalanche speeds." *Journal of Glaciology*, V36, p188-198
- McClung, D.M. and Mears, A.I.** (1991) "Extreme value prediction of snow avalanche runout." *Cold Regions Science and Technology*, V19, p163-175
- McClung, D.M. and Tweedy, J.** (1993) "Characteristics of avalanching: Kootenay Pass, British Columbia, Canada." *Journal of Glaciology*, V39, p316-322
- McClung, D.M. and Schaerer, P.** (1993) *The Avalanche Handbook The Mountaineers, Seattle*
- McGregor, G.R.** (1989) "Snow avalanche terrain of the Cragieburn Range, Central Canterbury, New Zealand." *New Zealand Journal of Geology and Geophysics* V32, p401-409
- McKittrick, L.R. and Brown, R.L.** (1993) "A statistical model for maximum avalanche run-out distances in southwest Montana." *Annals of Glaciology*, V18, p295-302
- McNulty, D. and Fitzharris, B.B.** (1980) "Winter avalanches activity and weather in a Canterbury alpine basin." *New Zealand Journal of Geology and Geophysics*, V23, p103-111
- Mears, A.I.** (1979) Colorado snow avalanche area studies and guidelines for avalanche-hazard planning *Colorado Geological Survey, Denver*

- Mears, A.I.** (1981) Design criteria for avalanche control structures in the runout zone *General Technical Report RM-84, Rocky Mountain Forest and Range Experiment Station, Forest Service US Department of Agriculture*
- Mears, A.I.** (1989) "Regional comparisons of avalanche-profile and run-out data." *Arctic and Alpine Research*, V21, p283-287
- Mears, A.I.** (1992) Snow-avalanche hazard analysis for land use planning and engineering *Colorado Geological Survey, Denver*
- Nixon, D.J. and McClung, D.M.** (1993) "Snow avalanche runout from two Canadian mountain ranges." *Annals of Glaciology*, V18, p1-6
- Norem, H., Irgens, F. and Schieldrop, B.** (1989) "Simulation of snow-avalanche flow in run-out zones." *Annals of Glaciology*, V13, p218-225
- Perla, R., Cheng, T.T. and McClung, D.M.** (1980) "A two-parameter model of snow avalanche motion." *Journal of Glaciology*, V26, p197-206
- Perla, R., Lied, K. and Kristensen, K.** (1984) "Particle simulation of snow avalanche motion." *Cold Regions Science and Technology*, V9, p191-202
- Rawlings, J.O.** (1988) *Applied Regression Analysis: A Research Tool Wadsworth, California*
- Roscoe, J.T. and Bryars, J.A.** (1971) "An investigation of the restraints with respect to sample size commonly imposed on the use of the chi-square statistic." *Journal of the American Statistical Association*, V66, p755-759
- Salway, R.A.** (1979) "Time series modelling of avalanche activity from meteorological data." *Journal of Glaciology*, V22, p513-528
- Schaerer, P.A.** (1967) "The amount of snow deposited at avalanche sites." *Proceedings of the Sapporo Conference, Japan, August 14th-19th 1966*, V1, 2, p1255-1260
- Schaerer, P.A.** (1973) "Terrain and vegetation of snow avalanche sites at Rogers Pass, British Columbia." *BC Geog. Series*, No.14, p215-222
- Schaerer, P.A.** (1977) "Analysis of snow avalanche terrain." *Canadian Geotechnical Journal*, V14, p281-287
- Schaerer, P.A.** (1984) "Measurements of the amount of snow brought down by avalanches." *Proceedings of the International Snow Symposium Workshop, Aspen*, p78-79
- Schaerer, P.A. and Fitzharris, B.B.** (1984) "Estimation of the mass of large snow avalanches." *Canadian Journal of Civil Engineering*, V11, p74-81
- Schaerer, P.A.** (1988) "The yield of avalanche snow at Rogers Pass, British Columbia, Canada." *Journal of Glaciology*, V34, p188-193

Schleiss, V.G. (1989) Rogers Pass snow avalanche atlas; Glacier National Park, BC, Canada
Environment Canada

Smith, L. (1973) "Identification of snow avalanche periodicity through interpretation of vegetative patterns in the North Cascades, Washington." *Methods of avalanche control on Washington mountain highways-Third Annual Report, Seattle, WA:Washington State Department of Highways*

Voight, V. (ed) (1990) Snow avalanche hazards and mitigation in the United States *National Academy Press*

Walsh, S.J., Butler, D.R., Brown, D.G. and Bian, L. (1990) "Cartographic modelling of snow avalanche path location within Glacier National Park, Montana." *Photogrammetric Engineering and Remote Sensing*, V56, p615-621

Walsh, J. and Butler, D.R. (1991) "Biophysical impacts of the morphological components of snow-avalanche paths, Glacier National Park, Montana." *ACSH-ASPRS Fall Convention, Atlanta, Georgia*

Young, C. (1985) The forests of British Columbia *Whitecap Books, North Vancouver*

APPENDIX 1 - FIELD REPORT

In this appendix I provide a description of all areas that were field checked, including all areas that were not included in the final data set. All areas are numbered (see bracketed number) and can be located on Figure A1.1.

Coast Mountains

The Duffey Lake (2) area had many paths with a large vertical drop and multiple starting zones. The area is densely vegetated, although logging prevented the location of many avalanche path tips. Avalanche frequency data were unavailable during field work, and so atlas information and field judgement were used to determine if the avalanche path should be included in the data set. When avalanche frequency data were available, several paths were rejected as they were of low-frequency. Many avalanche paths end at Cayoosh Creek or Duffey Lake and so prevented their inclusion.

The Bridge River (1) area had very few paths that could be selected. River terraces meant that many avalanches ran out on level ground, however these were on south facing slopes and so vegetation was sparse (also partly due to the close location to the interior plateau), so that, in many cases, no maximum runout could be defined. Many avalanche paths ended at Carpenter Lake and so prevented their use.

Other Coast Mountain areas include Bella Coola (fairly small) and the Stewart Region. These were regarded as too distant for one field season and so were rejected for practical reasons; however it is recommended that they be incorporated into any future study. The Stewart region contains a large number of well monitored avalanche paths.

Cascades

Allison Pass (3) was the only site visited in the Cascades and was a small avalanche area with many paths ending at the Nicolum River. Most paths were unusable, although several satisfactory paths were located. It was generally noted that the Cascades are a lot steeper than the Coast Mountains of British Columbia or the Canadian Rockies.

The Fraser Canyon (13) was briefly visited; although there were many high-frequency avalanche paths, they all ended at the Fraser River and so avalanche runout could not be located. The avalanche paths were steep and short. It was notable that in particularly rocky areas, most paths were found on open slopes rather than being channelised in gullies. The Coquihalla Highway was also visited, however this has mainly low-frequency paths, many of which impact on the adverse slope.

Columbia Mountains (incorporating the Monashees, Selkirks and Purcells)

For the Columbia Mountains I was able to make use of the frequency data provided by the Ministry of Transportation and Highways. The Kootenay Pass (8) area had avalanche paths that are steep and very frequent (up to several per year).

Blueberry-Paulson (4b) and Sheep Creek (4c) are very steep, canyon like terrain. Avalanche paths often ended at the creek. Grand Forks North (4a) had several useful paths, although many ended at the creek or were very low-frequency. Seven Mile Dam (4d) and Castlegar Bluffs (4e) were unusable due to urbanization.

Whitewater (5c) contained several useful paths. The avalanche path runout zones were located in a wide river valley. Several paths impacted on the adverse slope. The Vallican Bluffs (5b) paths all ended at Slocan River. Cape Horn Bluffs (5a) provided many very high-

frequency paths; however they all ended at Slocan Lake. The Fernie (6) region was rejected as all the paths ended at Elk River.

The New Denver-Kaslo (7a) area had many paths with large vertical drops. Field evidence suggested that these paths were of a low-frequency. Atlas information, dating back to 1954, confirmed the field evidence. Many avalanche paths ended at Carpenter Creek, Kaslo River, Bear Lake or Fish Lake. Lardeau (7b) and Coffee Creek (7c) had paths which ended at Kootenay Lake.

The Revelstoke-Mica (9a) area had most paths ending at Lake Revelstoke. At the upper end, some high-frequency paths ended in the steep river canyon of the Columbia River. Galena Pass-Beaton Road (9b) was a narrow gorge region, with a small river running through it. Several paths were useable, although many impacted on the adverse slope or ended at a small lake. The Greenslide (9c) area had paths which ended at Upper Arrow Lake. Three-Valley Gap (10b) had no useable paths as most ended at Griffin Lake and Three Valley Lake.

Glacier (10a) provided several paths; however many ended at the Illecilliewaet River and impacted on the adverse slope. The avalanche paths had large vertical drops and steep slopes. Avalanche paths in Rogers Pass (22) (a continuation of Glacier, but in Glacier National Park) had large vertical drops with many high-frequency avalanche paths. Most avalanche paths impacted on the adverse slope and so only several paths were useable. Toby Creek (11b) had several useful avalanche paths, many with large vertical drops.

Rockies

Kootenay National Park (17) had very few avalanche paths, most of which had large vertical drops and ended at Vermillion River. Event frequency allowed the selection of several paths. Golden East (11a) had very steep terrain and had many high event frequency avalanche paths; however most avalanche paths ended at the Kicking Horse River and so the path tip could not be located. Kicking Horse Pass (16) (in Yoho National Park) had steep terrain; however the braiding of the Kicking Horse River at this point, and urbanization, prevented any paths from being selected.

One path was selected from the Sunshine Creek (18) area in Banff National Park. This area had large vertical drops; however the valley bottom was v-shaped and so most paths impacted on the adverse slope. Several paths were selected from the Icefields Parkway (19) in Banff National Park.

Several paths were selected from the Icefields Parkway (20) in Jasper National Park. Many avalanche paths ended at rivers and so it was not possible to locate the path tip. The Maligne Lake Road (21) area, in Jasper National Park, had avalanche paths which ended in either Medicine Lake or Maligne River.

The Red Pass (12) area had avalanche paths with large vertical drops and were generally very low-frequency, although one path was selected.

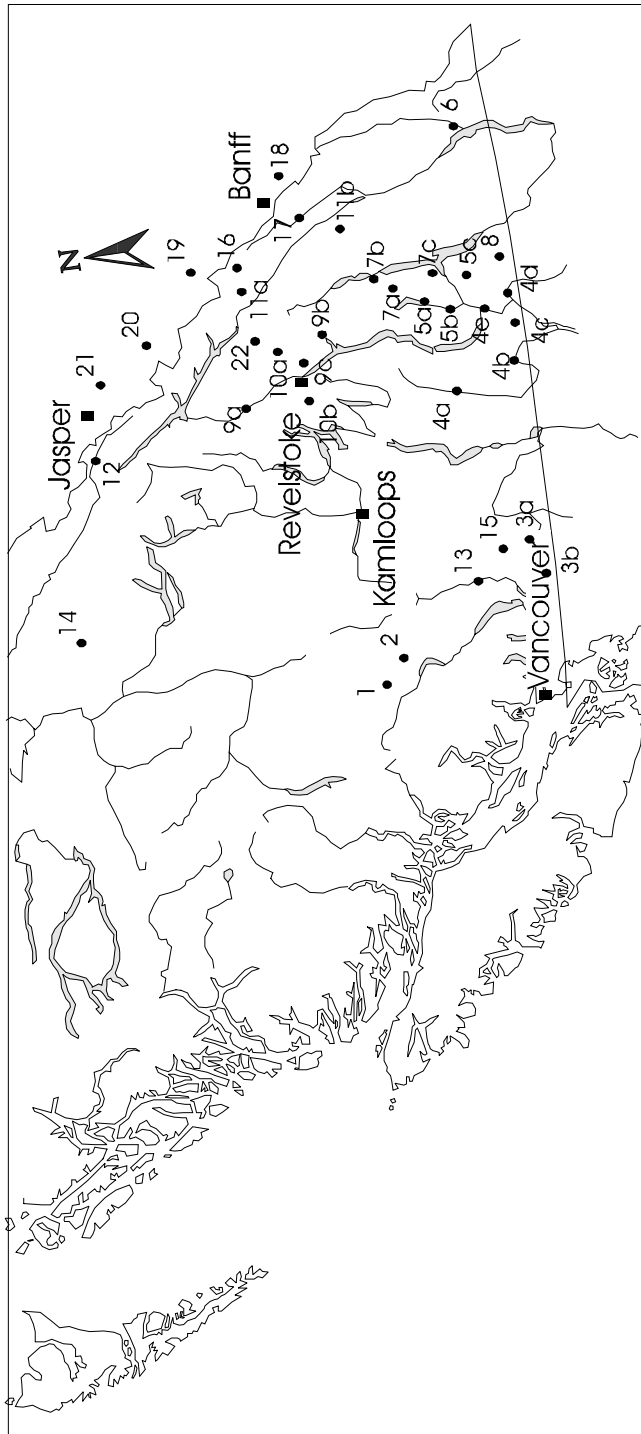


Figure A1.1 Location of field checked avalanche areas, monitored by the Ministry of Transportation and Highways or Parks Canada, within south-west British Columbia

APPENDIX 2 - AVALANCHE PATHS AND PHOTOGRAPHY

Path No	Roll No	Photo No	Map	Camera	CFL (mm)	Height (ft)	Date
W0.9	BC7106	168-169	82F/6	Zeiss 2	305	20000	31/8/68
KP20.2	BC5651	62-64	SP	ZE21162	152.433	23000	20/5/75
KP20.3							
KP20.4							
KP20.5							
KP21.2							
KP21.6							
KP21.7							
KP21.9							
KP22.0							
KP26.1	BC 5348	143-144	SP	RC8-355	153.35	24000	28/7/69
KP26.7							
KP26.8							
KP26.9							
KP27.1							
KP29.7	BC 5348	118-119	SP	RC8-355	153.35	24000	28/7/69
KP30.2							
KP30.4							
KP30.7							
KP30.8							
KP32.4							
GF38.0	BC79060	161-162	82E/8	122520	305.09	20340	28/6/79
BP37.8	BC 7582	188-189	82E/1	1103982	305.56	20000	24/7/74
BP42	BC 7582	175-176	82E/1	1103982	305.56	20000	24/7/74
BP43							

Path No	Roll No	Photo No	Map	Camera	CFL (mm)	Height (ft)	Date
BP44							
MD30.8	BC 5742	45-47	82M/8	124223	152.937		1/9/76
RP88	BC86088	241-245	82N/4-6	RC10	153.274	15000	7/8/86
RP94							
RP95							
RP107							
TC55.7	BC 5364	227-228	82K/8	RC8 355	153.35	24000	26/8/69
TC57.6							
TC58.3							
TC75.2	BC 7546	80-81	82K/8	110398	305.56	20000	14/8/73
TC75.3							
ND3.21	BC 5634	237-239	82K/3-82F/14	RC8	152.26	20000	25/9/74
ND3.5							
ND5.6							
G19.8	BC 7801	62-64	82N/4W	122520	305.57	28000	9/9/75
G20.0							
G23.0							
GP2.0	BC 90130	222-223	82K/12	124223	152.909	26000	12/8/75
GP2.6							
GP2.8							
GP4.01							

Table A2.1 Avalanche paths used in terrain analysis and their respective photography

W	Whitewater	(5c)	KP	Kootenay Pass	(8)
GF	Grand Forks North	(4a)	GP	Galena Pass	(9b)
BP	Blueberry-Paulson	(4b)	RP	Rogers Pass	(22)
MD	Mica Dam	(9a)	TC	Toby Creek	(11b)
ND	New Denver-Kaslo	(7a)	G	Glacier	(10a)

APPENDIX 3 - SUMMARY STATISTICS FOR LOW-FREQUENCY AVALANCHE PATH REGIONS

		CR n=127	WN n=127	CA n=52	CoR n=130	SN n=90	BC n=31	M n=26
α	mean	27.8	29.4	25.4	22.1	20.1	26.8	
	std	3.5	5.2	3.2	3.2	3.6	3.3	
	min	20.5	18.0	18.9	15.5	14.0	20.4	
	max	40.0	42.0	34.2	30.7	35.9	32.5	
β	mean	29.8	32.6	29.6	27.5	26.3	29.5	
	std	3.1	5.4	3.3	3.6	4.2	3.0	
	min	23.0	21.0	23.0	18.8	16.5	22.8	
	max	42.0	45.0	38.2	37.7	40.7	34.0	
δ	mean	5.5	6.4	5.2	5.1	4.8	5.5	
	std	5.3	3.5	3.1	3.4	2.7	3.6	
	min	-21.5	0	0	-2.9	0	-5	
	max	20.6	16.0	9.5	10.2	9.0	14.1	
H	mean	869	827	765	543	429	903	248
	std	268	255	247	227	239	313	123
	min	350	342	320	128	104	426	68
	max	1960	1539	1400	1134	1145	1915	553
Δx	mean	168	224	302	334	354	229	66
	std	131	170	166	185	223	202	102
	min	-190	-119	80	76	107	0	-87
	max	524	823	790	1200	1433	1150	340
$\Delta x / X_{\beta}$	mean	0.114	0.176	0.25	0.406	0.49	0.159	
	std	0.1	0.111	0.14	0.262	0.26	0.115	
	min	-0.185	-0.121	0.07	0.07	0.15	0	
	max	0.404	0.52	0.66	1.57	1.35	0.559	

(caption next page)

Table A3.1 Summary statistics for low-frequency avalanche path regions, with the following notation

CR	Canadian Rockies	WN	western Norway
CA	Coastal Alaska	CoR	Colorado Rockies
SN	Sierra Nevada	BC	British Columbia Coast Mountains
M	south-west Montana		